

LHC PHYSICS AND COSMOLOGY

N.E. MAVROMATOS

*King's College London, Department of Physics,
Strand, London WC2R 2LS, U.K.
E-mail: Nikolaos.Mavromatos@kcl.ac.uk*

In these Lectures I review possible constraints on particle physics models, obtained by means of combining the results of collider measurements with astrophysical data. I emphasize the theoretical-model dependence of these results. I discuss supersymmetric dark matter constraints at colliders (mainly LHC) in various theoretical contexts: the standard Cosmological-Constant-Cold-Dark-Matter (Λ CDM) model, (super)string-inspired ones and non-equilibrium relaxation dark energy models. I then investigate the capability of LHC measurements in asserting whether supersymmetric matter (if discovered) constitutes part, or all, of the astrophysical dark matter. I also discuss prospects for improving the constraints in future precision facilities, such as the International Linear Collider.

1. Introduction

In the past decade we have witnessed spectacular progress in precision measurements in astrophysics as a result of significant improvements in terrestrial and extraterrestrial instrumentation. From the point of view of interest to particle physics, the most spectacular claims from astrophysics came in 1999 from the study of distant (redshifts $z \sim 1$) supernovae (SNe) of type Ia by two independent groups¹. These observations pointed towards a current era acceleration of our Universe, something that could be explained either by a non-zero cosmological *constant* in a Friedman-Robertson-Walker-Einstein Universe, or in general by a non-zero *dark energy* component, which could even be relaxing to zero (the data are consistent with this possibility). In the past five years² many more distant ($z > 1$) supernovae have been discovered, exhibiting similar features as the previous measurements, thereby supporting the geometric interpretation of the acceleration of the Universe today, and arguing against the nuclear physics or intergalactic dust effects.

Moreover, there is strong additional evidence from quite different in origin and thus independent astrophysical observations, those associated with

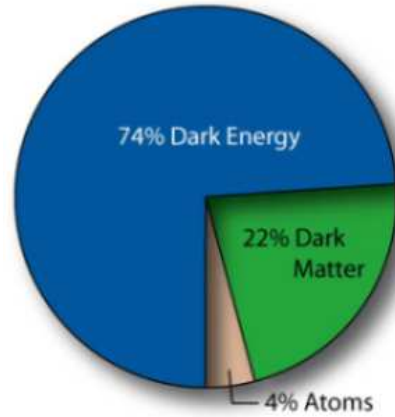


Figure 1. The energy content of our Universe as obtained by fitting data of WMAP satellite. The chart is in perfect agreement with earlier claims made by direct measurements of a current era acceleration of the Universe from distant supernovae type Ia (courtesy of <http://map.gsfc.nasa.gov/>).

the WMAP measurements of the cosmic microwave background radiation (CMB) ³, as well as baryon acoustic oscillations measurements ⁴. After three years of running, WMAP measured CMB anisotropies to an unprecedented accuracy of billionth of a Kelvin degree, thereby correcting previous measurements by the Cosmic Background Explorer (COBE) satellite ⁵ by several orders of magnitude. This new satellite experiment, therefore, opened up a new era for astro-particle physics, given that such accuracies allow for a determination (using best fit models of the Universe) of cosmological parameters ⁶, and in particular cosmological densities, which, as we shall discuss in this review, is quite relevant for constraining models of particle physics to a significant degree. All these measurements point towards the fact that (more than) 73 % of the Universe vacuum energy consists of a dark (unknown) energy substance, in agreement with the (preliminary) supernovae observations (see fig. 1). This claim, if true, could revolutionize our understanding of the basic physics governing fundamental interactions in Nature. Indeed, only a few years ago, particle theorists were trying to identify (alas in vain!) an exact symmetry of nature that could set the cosmological constant (or more generally the vacuum energy) to zero. Now, astrophysical observations point to the contrary. The WMAP satellite experiment determined the most important cosmological parameters that could be of relevance to particle physicists, namely ⁶: the Hubble constant, and

thus the age of the Universe, the thickness of the last scattering surface, the dark energy and dark matter content of the Universe (to an unprecedented accuracy) (c.f. figure 1), confirming the earlier claims from supernovae Ia data ¹, and provided evidence for early re-ionization ($z \sim 20$), which, at least from the point of view of large scale structure formation, excludes Warm Dark Matter particle theory models. Its measurements have been independently confirmed recently by Baryon Oscillation measurements ⁴.

In this review I shall first describe briefly the above-mentioned astrophysical measurements, and then use them to constrain ⁷ some particle physics supersymmetric models, in particular (i) the minimally supersymmetric model, constrained by its embedding in a minimal supergravity model (mSUGRA) ⁸, (ii) a class of string-inspired cosmologies ⁹, with non-trivial dilaton and/or moduli fields, and (iii) a class of stringy relaxation dark energy models ¹⁰. I shall give a critical discussion on the derived constraints, and their strong theoretical-model dependence, and discuss the capability of observing Supersymmetry in colliders after the latest astrophysical data. In this respect I will also discuss the importance of the $g_\mu - 2$ experiments of the muon gyromagnetic ratio, in light of some very recent (2006) results ¹¹, pointing towards a discrepancy between the measured $g_\mu - 2$ value from the one calculated within the standard model.

2. Astrophysical Measurements and Facts

On Large scales our Universe looks isotropic and homogeneous. A good formal description, which does not depend on the detailed underlying microscopic model, is provided by the Robertson-Walker (RW) metric, according to which the geometry of the Universe is described by means of the following space-time invariant element ¹²:

$$ds^2 = -dt^2 + a(t)^2 R_0^2 \left[\frac{dr^2}{1 - k r^2} + r^2 (d\theta^2 + \sin^2\theta d\varphi^2) \right] \quad (2.1)$$

where $a(t) = \frac{R(t)}{R_0} = \frac{1}{1+z}$ is the scale factor, $H \equiv \frac{\dot{a}}{a}$ is the Hubble Parameter, t is the Cosmological Observer time, R_0 denotes the present-day scale factor, z is the redshift, k denotes the *Spatial Curvature*, which (by normalization) can take on the values: $k=0$ for a flat Universe (required by inflationary models), $k=1$ for a closed and $k=-1$ for an open Universe. In this section we shall outline the main Cosmological Measurements and the pertinent quantities, of interest to us in these Lectures. For more details we refer the reader to the literature ¹².

2.1. Model Independent (Geometric) Considerations

An important quantity, which we shall make extensive use of in the following, when we use astrophysical data to constrain theoretical models, is the so-called *Luminosity Distance*, d_L , defined as: $d_L = \sqrt{\frac{\mathcal{L}}{4\pi\mathcal{F}}}$, where \mathcal{L} is the energy per unit time emitted by the source, at the source's rest frame, and \mathcal{F} is the flux measured by detector, i.e. the energy per unit time per unit area measured by the detector. Taking into account the time dilation induced by the expansion of the Universe: $\delta t_{\text{detector}} = (\delta t)_{\text{source}}(1+z)$, as well as as the cosmic red-shift, i.e. the fact that there is a reduced energy of photons at the detector as compared with that at emission from the source, we obtain: $\mathcal{F} = \frac{\mathcal{L}}{4\pi a(t_0)^2 r_1^2 (1+z)^2}$.

Another very commonly used quantity in Astrophysics is the *Angular Diameter*, which is defined as follows: A celestial object (cluster of galaxies etc.) has proper diameter D at $r = r_1$ and emits light at $t = t_1$. The observed angular diameter by a detector at $t = t_0$ is: $\delta = \frac{D}{a(t_1)r_1}$. From this one defines the *Angular Diameter Distance*: $d_A = \frac{D}{\delta} = a(t_1)r_1 = d_L(1+z)^2$.

The *Horizon Distance* (beyond which light cannot reach us) is defined as: $ds^2 = 0 = dt^2 - a^2(t) \left(\frac{dr^2}{1-kr^2} + r^2 d\Omega^2 \right)$. For radial motion of light, pertinent to most observations, along null geodesics $ds^2 = 0$, we have: $\int_0^t \frac{dt'}{a(t')} = \int_0^{r_H} \frac{dr}{\sqrt{1-kr^2}}$ from which $d_H = a(t) \int_0^{r_H} \sqrt{g_{rr}} = a(t) \int_0^t \frac{dt'}{a(t')}$. In Standard Cosmology $d_H \sim t_{\text{Age}} < \infty$ due to the finite age of the Universe, i.e. there is an Horizon.

The above quantities are related among themselves¹², as follows from the cosmic redshift phenomenon, the fact that photons follow null geodesics $ds^2 = 0$ etc. These leads to relations among H_0, d_L and the redshift z , which are model independent, and they follow from pure geometrical considerations relying on the assumption of a RW homogeneous and isotropic cosmology. In the next subsection we discuss how a specific dynamical model of the Universe affects the cosmological measurements. In particular, as we shall show, model dependence is hidden inside the details of the dependence of the Hubble parameter on the various components of the Universe's energy budget. This property is a consequence of the pertinent dynamical equations of motion of the gravitational field.

2.2. Cosmological Measurements: Model Dependence

Within the standard General-Relativistic framework, according to which the dynamics of the gravitational field is described by the Einstein-Hilbert action, the gravitational (Einstein) equations in a Universe with cosmological constant Λ read: $R_{\mu\nu} - \frac{1}{2}g_{\mu\nu}R + g_{\mu\nu}\Lambda = 8\pi G_N T_{\mu\nu}$, where G_N is (the four-dimensional) Newton's constant, $T_{00} = \rho$ is the energy density of matter, and $T_{ii} = a^2(t)p$ with p = the pressure, and we assumed that the Universe and matter systems behave like ideal fluids in a co-moving cosmological frame, where all cosmological measurements are assumed to take place. From the RW metric (2.1), we arrive at the Friedman equation:

$$3 \left(\frac{\dot{a}}{a} \right)^2 + 3 \frac{k}{a^2} - \Lambda = 8\pi G_N \rho \quad (2.2)$$

From this equation one obtains the expression for the Critical density (i.e. the total density required for flat $k = \Lambda = 0$ Universe): $\rho_c = \frac{3}{8\pi G_N} \left(\frac{\dot{a}}{a} \right)^2$.

From the dynamical equation (2.2) one can obtain various relations between the Hubble parameter $H(z)$, the luminosity distance d_L , the deceleration parameter $q(z)$ and the energy densities ρ at various epochs of the Universe. For instance, for matter dominating flat ($k = 0$) Universes with $\Lambda > 0$ and various (simple, z -independent) equations of state $p = w_i \rho$, ($w_r = 1/3$ (radiation), $w_m = 0$ (matter-dust), $w_\Lambda = -1$ (cosmological constant (de Sitter))) we have for the Hubble parameter:

$$H(z) = H_0 \left(\sum_i \Omega_i (1+z)^{3(1+w_i)} \right)^{1/2} \quad (2.3)$$

with the notation: $\Omega_i \equiv \frac{\rho_i^0}{\rho_c}$, $i = r$ (adiation), m (atter), Λ , ...

For the deceleration parameter we have at late eras, where radiation is negligible : $q(z) \equiv -\frac{\ddot{a}a}{\dot{a}^2} = \left(\frac{H_0}{H(z)} \right)^2 \left(\frac{1}{2}\Omega_m(1+z)^3 - \Omega_\Lambda \right)$, with $q_0 = \frac{1}{2}\Omega_m - \Omega_\Lambda$. Thus, it becomes evident that Λ acts as ‘‘repulsive’’ gravity, tending to accelerate the Universe currently, and eventually dominates, leading to an eternally accelerating de Sitter type Universe, with a future cosmic horizon. At present in the data there is also evidence for past deceleration ($q(z) > 0$, for some $z > z^* > 0$), which is to be expected if the dark energy is (almost) constant, due to matter dominance in earlier eras: $q(z) > 0 \Rightarrow (1+z)^3 > 2\Omega_\Lambda/\Omega_m \Rightarrow z > z^* = \left(\frac{2\Omega_\Lambda}{\Omega_m} \right)^{1/3} - 1$.

Finally, for the luminosity distance we obtain the important relation:

$d_L = (1+z) \int_{t_1}^{t_0} \frac{a(t_0)dt}{a(t)} = -(1+z) \int_{a(t_1)}^{a(t_0)} \frac{d(\frac{a(t_0)}{a})}{(\frac{\dot{a}}{a})}$, from which

$$d_L = (1+z) \int_0^z \frac{dz}{H(z)} \quad (2.4)$$

We shall use this relation in the following, in order to constrain various theoretical cosmological models by means of astrophysical observations.

2.3. *Supernovae Ia Measurements of Cosmic Acceleration*

Type Ia Supernovae (SNe) behave as Excellent Standard Candles, and thus can be used to measure directly the expansion rate of the Universe at high redshifts ($z \geq 1$) and compare it with the present rate, thereby providing direct information on the Universe's acceleration. SNe type Ia are very bright objects, with absolute magnitude $M \sim 19.5$, typically comparable to the brightness of the entire host galaxy! This is why they can be detected at high redshifts $z \sim 1$, i.e. 3000 Mpc , $1 \text{ pc} \sim 3 \times 10^{16} \text{ m}$. Detailed studies of the luminosity profile^{1,2} of each SNe suggests a strong relation between the width of the light curve and the absolute luminosity of SNe. This implies an accurate determination of its absolute luminosity. For each supernova one measures an effective (rest frame) magnitude in blue wavelength band, m_B^{eff} , which is then compared with the theoretical expectation (depending on the underlying model for the Universe) to yield information on the various Ω^i . The larger the magnitude the dimmer the observed SNe.

To understand the pertinent measurements recall the relation between the observed (on Earth) and emitted wavelengths $\lambda_{\text{obs}} = (1+z)\lambda_{\text{emit}}$, as a result of the cosmic redshift phenomenon. In a magnitude-redshift graph, if nothing slowed down matter blasted out of the Big Bang, we would expect a straight line. The data from High-redshift ($z \sim 1$) SNe Ia, showed that distant SNe lie slightly above the straight line. Thus they are moving away slower than expected. So at those early days ($z \sim 1$) the Universe was expanding at a slower rate than now. *The Universe accelerates today!* In such measurements, one needs the Hubble-Constant-Free Luminosity Distance: $\mathcal{D}_L(z; \Omega_M, \Omega_\Lambda) = \frac{H_0}{c} d_L$, $d_L \equiv \sqrt{\frac{L}{4\pi F}}$, with L the Intrinsic Luminosity of source, F the Measured Flux. In Friedman models \mathcal{D}_L is parametrically known in terms of Ω_M, Ω_Λ . An important quantity used in measurements is the Distance Modulus $m - M$, where $m = M + 25 + 5 \log \left(\frac{d_L}{1 \text{ Mpc}} \right) = \mathcal{M} + 5 \log \mathcal{D}_L$, with m =Apparent Magnitude of the Source, M the Absolute Magnitude, and $\mathcal{M} \equiv M - 5 \log H_0 + 25$ the fit parameter. Comparison of theoretical expectations

with data restricts Ω_M, Ω_Λ . An important point to notice is that for fixed redshifts z the eqs. $\mathcal{D}_L(z; \Omega_M, \Omega_\Lambda) = \text{constant}$ yields *degeneracy curves* \mathcal{C} in the Ω -plane, of small curvature to which one associates a small slope, with the result that even very accurate data can at best select a narrow strip in Ω -plane parallel to \mathcal{C} . The results (2004) are summarized in figure 2. In the early works (1999) it was claimed that the best

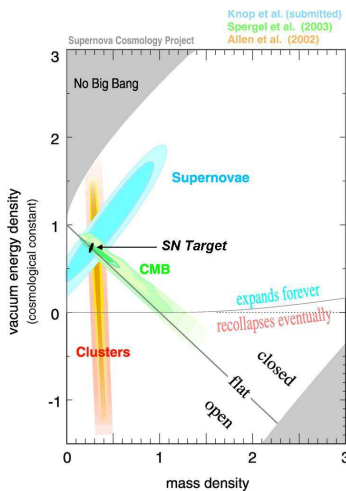


Figure 2. Supernovae (and other) measurements on the Universe's energy budget.

fit model, that of a FRW Universe with matter and cosmological constant for $z \leq 3$ (where the SNe data are valid) yields the following values: $0.8\Omega_M - 0.6\Omega_\Lambda \simeq -0.2 \pm 0.1$, for $\Omega_M \leq 1.5$. Assuming a flat model ($k=0$) the data imply: $\Omega_M^{Flat} = 0.28_{-0.08}^{+0.09}$ (1σ stat) $_{-0.04}^{+0.05}$ (identified syst.), that is the *Universe accelerates today*

$$q_0 = \frac{1}{2}\Omega_M - \Omega_\Lambda \simeq -0.6 < 0$$

Further support on these results comes, within the SNe measurement framework, from the recent (> 2004) discovery ², by Hubble Space Telescope, ESSENCE and SNLS Collaborations, of more than 100 high- z ($2 > z \geq 1$) supernovae, pointing towards the fact that for the past 9 billion years the energy budget of the Universe is dominated by an approximately constant dark energy component.

2.4. CMB Anisotropy Measurements by WMAP1,3

After three years of running, WMAP provided a much more detailed picture of the temperature fluctuations than its COBE predecessor, which can be analyzed to provide best fit models for cosmology, leading to severe constraints on the energy content of various model Universes, useful for particle physics, and in particular supersymmetric searches. Theoretically¹², the temperature fluctuations in the CMB radiation are attributed to: (i) our velocity w.r.t cosmic rest frame, (ii) gravitational potential fluctuations on the last scattering surface (Sachs-Wolf effect), (iii) Radiation field fluctuations on the last scattering surface, (iv) velocity of the last scattering surface, and (v) damping of anisotropies if Universe re-ionizes after decoupling. A Gaussian model of fluctuations¹², favored by inflation, is in very good agreement with the recent WMAP data (see figure 3). The perfect fit of the first few peaks to the data allows a precise determination of the total density of the Universe, which implies its spatial flatness. The various

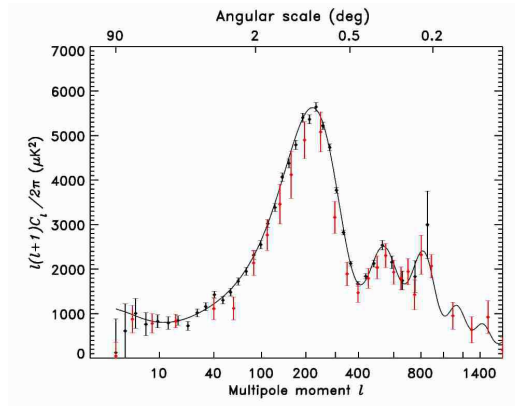


Figure 3. Red points (larger errors) are previous measurements. Black points (smaller errors) are WMAP measurements (G. Hinshaw, *et al.* arXiv:astro-ph/0302217).

peaks in the spectrum of fig. 3 contain interesting physical signatures:

- (i) The angular scale of the first peak determines the curvature (but not the topology) of the Universe.
- (ii) The second peak –truly the ratio of the odd peaks to the even peaks– determines the reduced baryon density.
- (iii) The third peak can be used to extract information about the dark matter (DM) density (this is a model-dependent result, though –

standard local Lorentz invariance assumed, see discussion in later sections on Lorentz-violating alternative to dark matter models).

The measurements of the WMAP ⁶ on the cosmological parameters of interest to us here are given in ⁶, and reviewed in ⁷. The WMAP results constrain severely the equation of state $p = w\rho$ (p =pressure), pointing towards $w < -0.78$, if one fits the data with the assumption $-1 \leq w$ (we note for comparison that in the scenarios advocating the existence of a cosmological *constant* one has $w = -1$). Many quintessence models can easily satisfy the criterion $-1 < w < -0.78$, especially the supersymmetric ones, which we shall comment upon later in the article. Thus, at present, the available data are not sufficient to distinguish the cosmological constant model from quintessence (or more generally from relaxation models of the vacuum energy). The results lead to the chart for the energy and matter content of our Universe depicted in figure 1, and are in perfect agreement with the Supernovae Ia Data ¹. The data of the WMAP satellite lead to a new determination of $\Omega_{\text{total}} = 1.02 \pm 0.02$, where $\Omega_{\text{total}} = \rho_{\text{total}}/\rho_c$, due to high precision measurements of secondary (two more) acoustic peaks as compared with previous CMB measurements (c.f. figure 3). Essentially the value of Ω is determined by the position of the first acoustic peak in a Gaussian model, whose reliability increases significantly by the discovery of secondary peaks and their excellent fit with the Gaussian model ⁶.

Finally we mention that the determination of the cosmological parameters by the WMAP team ⁶, after three years of running. favors, by means of best fit procedure, *spatially flat* inflationary models of the Universe ¹³. In general, WMAP gave values for important inflationary parameters, such as the running spectral index, $n_s(k)$, of the primordial power spectrum of scalar density fluctuations $\delta_{\vec{k}}$ ¹⁴ $P(k) \equiv |\delta_{\vec{k}}|^2$. The running scalar spectral index $n_s(k)$ is $n_s(k) = \frac{d \ln P(k)}{d \ln k}$, where k is the co-moving scale. Basically inflation implies $n_s = 1$. WMAP measurements yield $n_s = 0.96$, thus favoring Gaussian primordial fluctuations, as predicted by inflation. For more details we refer the reader to the literature ^{6,7}.

2.5. *Baryon Acoustic Oscillations (BAO)*

Further evidence for the energy budget of the Universe is obtained by Detection of the baryon acoustic peak in the large-scale correlation function of SDSS luminous red galaxies ⁴. The underlying Physics of BAO can be understood as follows: Because the universe has a significant fraction of baryons, cosmological theory predicts that the acoustic oscillations (CMB)

in the plasma will also be imprinted onto the late-time power spectrum of the non-relativistic matter: from an initial point perturbation common to the dark matter and the baryons, the dark matter perturbation grows in place while the baryonic perturbation is carried outward in an expanding spherical wave. At recombination, this shell is roughly 150 Mpc in radius. Afterwards, the combined dark matter and baryon perturbation seeds the formation of large-scale structure. Because the central perturbation in the dark matter is dominant compared to the baryonic shell, the acoustic feature is manifested as a small single spike in the correlation function at 150 Mpc separation ⁴.

The acoustic signatures in the large-scale clustering of galaxies yield three more opportunities to test the cosmological paradigm with the early-universe acoustic phenomenon:

- (1) They would provide smoking-gun evidence for the theory of gravitational clustering, notably the idea that large-scale fluctuations grow by linear perturbation theory from $z \sim 1000$ to the present;
- (2) they would give another confirmation of the existence of dark matter at $z \sim 1000$, since a fully baryonic model produces an effect much larger than observed;
- (3) they would provide a characteristic and reasonably sharp length scale that can be measured at a wide range of redshifts, thereby determining purely by geometry the angular-diameter-distance-redshift relation and the evolution of the Hubble parameter.

In the current status of affairs of the BAO measurements it seems that there is an underlying-theoretical-model dependence of the interpretation of the results, as far as the predicted energy budget for the Universe is concerned. This stems from the fact that for small deviations from $\Omega_m = 0.3$, $\Omega_\Lambda = 0.7$, the change in the Hubble parameter at $z = 0.35$ is about half of that of the angular diameter distance. Eisenstein *et al.* in ⁴ modelled this by treating the dilation scale as the cubic root of the product of the radial dilation times the square of the transverse dilation. In other words, they defined

$$D_V(z) = \left[D_M(z)^2 \frac{cz}{H(z)} \right]^{1/3}, \quad H = H_0 \left(\sum_i \Omega_i (1+z)^{3(1+w_i)} \right)^{1/2} \quad (2.5)$$

where $H(z)$ is the Hubble parameter and $D_M(z)$ is the co-moving angular diameter distance. As the typical redshift of the sample is $z = 0.35$, we quote the result ⁴ for the dilation scale as $D_V(0.35) = 1370 \pm 64$ Mpc. The BAO measurements from Large Galactic Surveys and their results

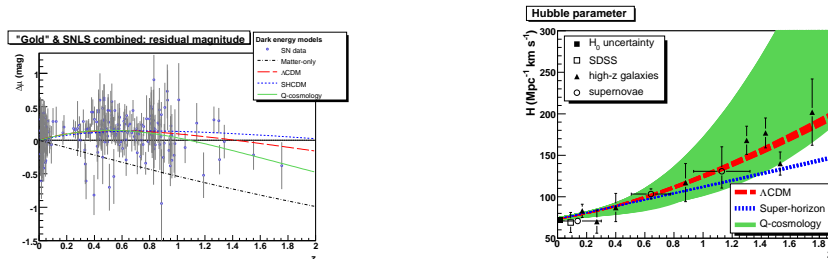


Figure 4. Left: Residual magnitude versus redshift for supernovae from the ‘gold’ and the SNLS datasets for various cosmological models. Right: The Hubble-parameter vs. redshift relation for these models and observational data. The bands represent 68% confidence intervals derived by the SN analysis for the standard Λ CDM, the super-horizon (no DE) and the Q -cosmology models. The black rectangle shows the WMAP3 estimate for H_0 , the squares show the measurements from SDSS galaxies, the triangles result from high- z red galaxies, and the circles correspond to a combined analysis of supernovae data (from [16]).

for the dark sector of the Universe are consistent with the WMAP data, as far as the energy budget of the Universe is concerned, but the reader should bear in mind that they based their parametrization on standard FRW cosmologies, so the consistency should be interpreted within that theory framework.

2.6. Measuring $H(z)$: an important constraint on models

The previous results, based on SNe, CMB and BAO measurements, relied on the standard FRW Cosmological model for the Universe as the underlying theory. However, in modern approaches to (quantum) gravity, such as brane and string theories, the underlying dynamics may no longer be described by the simple Einstein-Hilbert action. One may have extra fields, such as the dilaton or moduli fields in theories with extra dimensions, plus higher order curvature terms which could become important in the early Universe. Moreover, there have been suggestions in the literature¹⁵ that the claimed Dark Energy may not be there, but simply be the result of temperature fluctuations in a (flat) Universe filled with matter $\Omega_M = 1$ (“super-horizon model”). All such alternative theories should be tested against each one of the above-mentioned categories of measurements together with an independent measurement of the behavior of the Hubble parameter vs. the redshift $H(z)$, the latter coming from large galactic surveys. This latter measurement provides an *important constraint* which

could differentiate among the potential Dark Energy (DE)/Dark Matter (DM) models and their alternatives. This extra measurement has the potential of ruling out alternative models (to DM and DE) that otherwise fit the supernova data alone (in a m_{eff} vs z plot). This happens, for instance, with the super-horizon model of ¹⁵. I mention in passing that other non-equilibrium stringy cosmologies ¹⁰, with relaxing to zero dark energy (quintessence-like due to the dilaton field) survive at present this constraint, as illustrated in figure 4. For more details I refer the reader to ¹⁶ and references therein.

2.7. Cosmic Coincidence and Cosmological Constant Issues

There may be several possible explanations regarding the Dark Energy part of the Universe's energy budget:

(i) The dark energy is an ‘‘Honest’’ Cosmological Constant $\Lambda \sim 10^{-122} M_{\text{Pl}}^4$, strictly unchanging through space and time. This has been the working hypothesis of many of the best fits so far, but I stress it is *not* the only explanation consistent with the data.

(ii) Quintessence: The Cosmological constant is mimicked by a slowly-varying field, ϕ , whose time until it reaches its potential minimum is (much) longer than the Age of Universe. Simplest Quintessence models assume exponential potentials $V(\phi) \sim e^\phi$. In such a case the pertinent equation of state reads: $w = \frac{\frac{(\dot{\phi})^2}{2} - V(\phi)}{\frac{(\dot{\phi})^2}{2} + V(\phi)}$. For $\phi = -2\ln t$ one has a relaxing-to-zero vacuum energy $\Lambda(t) \sim \text{const}/t^2$ (in Planck units), of the right order of magnitude today. Such a situation could be met ¹⁰ in some models of string theory, where the rôle of the quintessence field could be played by the dilaton ¹⁷, i.e. the scalar field of the string gravitational multiplet.

(iii) Einstein-Friedman model is incorrect, and one could have modifications in the gravitational law at galactic or supergalactic scales. Models of this kind have been proposed as alternatives to dark matter, for instance Modified Newtonian Dynamics (MOND) by Milgrom ¹⁸, and its field theory version by Bekenstein ¹⁹, known as Tensor-Vector-Scalar (TeVeS) theory, which however, is Lorentz Violating, as it involves a preferred frame. Other modifications from Einstein theory, which however maintain Lorentz invariance of the four-dimensional world, could be brane models for the Universe, which are characterized by non-trivial, and in most cases time dependent, vacuum energy. It should be noted that such alternative models may lead to completely different energy budget ^{20,21}. We shall discuss one such case of a non-critical string inspired (non-equilibrium, relaxation) cosmology (Q-

cosmology) in a subsequent section, where we shall see that one may still fit the astrophysical data with exotic forms of “dark matter”, not scaling like dust with the redshift at late epochs, and different percentages of dark (dilaton quintessence) energy (c.f. also fig. 4).

Given that from most of the standard best fits for the Universe it follows that the energy budget of our Cosmos today is characterized by 73 – 74% vacuum energy, i.e. an energy density of order $\rho_{vac} \simeq (10^{-3} \text{ eV})^4 = 10^{-8} \text{ erg/cm}^3$, and about 27 – 26% matter (mostly dark), this implies *the Coincidence Problem*: “The vacuum energy density today is approximately equal (in order of magnitude) to the current matter density.” As the Universe expands, this relative balance is lost in models with a cosmological constant, such as the standard Λ CDM model, since the matter density scales with the scale factor as $\frac{\Omega_\Lambda}{\Omega_M} = \frac{\rho_\Lambda}{\rho_M} \propto a^3$. In this framework, at early times we have that the Vacuum Energy is much more suppressed as compared with that of Matter and Radiation, while at late times it dominates. There is only one brief epoch for which the transition from domination of one component to the other can be witnessed, and this epoch, according to the Λ CDM model, happened to be the present one! This calls for a microscopic Explanation, which is still lacking.

The smallness of the value of the Dark Energy today is another big mystery of particle physics. For several years the particle physics community thought that the vacuum energy was exactly zero, and in fact they were trying to devise microscopic explanations for such a vanishing by means of some symmetry. One of the most appealing, but eventually failed in this respect, symmetry justifications for the vanishing of the vacuum energy was that of *supersymmetry* (SUSY): if unbroken, supersymmetry implies strictly a vanishing vacuum energy, as a result of the cancelation among boson and fermion vacuum-energy contributions, due to opposite signs in the respective quantum loops. However, this cannot be the correct explanation, given that SUSY, if it is to describe Nature, must be broken below some energy scale M_{susy} , which should be higher than a few TeV, as partners have not been observed as yet. In broken SUSY theories, in four dimensional space times, there are contributions to vacuum energy $\rho_{vac} \propto \sim \hbar M_{\text{susy}}^4 \sim (\text{few TeV})^4$, which is by far greater than the observed value today of the dark energy $\Lambda \sim 10^{-122} M_P^4$, $M_P \sim 10^{19} \text{ GeV}$. Thus, SUSY does not solve the *Cosmological Constant Problem*, which at present remains one of the greatest mysteries in Physics.

In my opinion, the smallness today of the value of the “vacuum” energy density might point towards a relaxation problem. Our world may have

not yet reached equilibrium, from which it departed during an early-epoch cosmically catastrophic event, such as a Big Bang, or—in the modern version of string/brane theory—a collision between two brane worlds. This non equilibrium situation might be expressed today by a quintessence like exponential potential $\exp(\phi)$, where ϕ could be the dilaton field, which in some models¹⁰ behave at late cosmic times as $\phi \sim -2\ln t$. This would predict a vacuum energy today of order $1/t^2$, which has the right order of magnitude, if t is of order of the Age of the Universe, i.e. $t \sim 10^{60}$ Planck times. Supersymmetry in such a picture may indeed be a symmetry of the vacuum, reached asymptotically, hence the asymptotic vanishing of the dark energy. SUSY breaking may not be a spontaneous breaking but an *obstruction*, in the sense that only the excitation particle spectrum has mass differences between fermions and bosons. To achieve phenomenologically realistic situations, one may exploit²² the string/brane framework, by compactifying the extra dimensions into manifolds with non-trivial “fluxes” (these are not gauge fields associated with electromagnetic interactions, but pertain to extra-dimensional unbroken gauge symmetries characterizing the string models). In such cases, fermions and bosons couple differently, due to their spin, to these flux gauge fields (a sort of generalized “Zeeman” effects). Thus, they exhibit mass splittings proportional to the square of the “magnetic field”, which could then be tuned to yield phenomenologically acceptable SUSY-splittings, while the relaxation dark energy has the cosmologically observed small value today. In such a picture, SUSY is needed for stability of the vacuum, although today, in view of the landscape scenarios for string theory, one might not even have supersymmetric vacua at all. However, there may be another reason why SUSY could play an important physical rôle, that of dark matter. I now come to discuss this important issue, mainly from a particle physics perspective.

3. Dark Matter (DM)

In this section I will discuss issues pertaining to dark matter and supersymmetry. I will first make the case for Dark Matter, starting historically from discrepancies concerning rotational curves of galaxies. Then I will move to describe possible candidates, and based on standard models for cosmology to exclude many of them, by means of WMAP data, arguing that supersymmetric dark matter remains compatible with such data. I will again emphasize, however, the model dependence of such conclusions. Then I will proceed to discuss supersymmetric particle physics constraints

in various frameworks by describing the underlying general framework for calculating thermal dark matter relics and compare them with WMAP data. For a more complete discussion on direct searches for dark matter the reader is referred to ²³, and references therein.

3.1. *The Case for DM*

Dark Matter (DM) is defined as a Non luminous massive matter, of unknown composition, that does not emit or reflect enough electromagnetic radiation to be observed directly, but whose presence can be inferred from gravitational effects on visible matter. Observed phenomena consistent with the existence of dark matter are:

- (i) rotational speeds of galaxies and orbital velocities of galactic clusters,
 - (ii) gravitational lensing of background objects by galaxy clusters such as the Bullet cluster of galaxies, and
 - (iii) the temperature distribution of hot gas in galaxies and clusters of galaxies.
- (iv) As we have seen, DM also plays a central role in structure formation and galaxy evolution, and has measurable effects on the anisotropy of the cosmic microwave background, especially the third peak in the anisotropy spectrum (c.f. fig. 3).

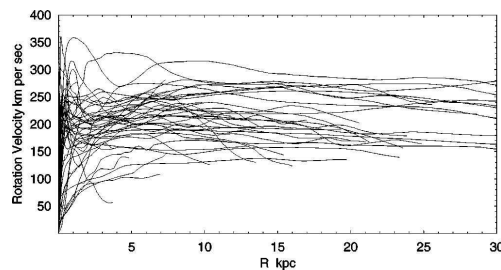


Figure 5. Collage of Rotational Curves of nearby spiral galaxies obtained by combining Doppler data from CO molecular lines for the central regions, optical lines for the disks, and HI 21 cm line for the outer (gas) disks. Graph from Y. Sofue and V. Rubin (Annual Review of Astronomy and Astrophysics, Volume 31 (c)2001, 127).

Historically, the first evidence for DM came ²⁴ from discrepancies concerning the Rotational Curves (RC) of Galaxies. If all matter were luminous then the rotational speed of the galactic disc would fall with the (radial) distance r from the center as $v(r) \sim r^{-1/2}$ but observations show that $v(r) \sim \text{const}$, as seen clearly in figure 5, where the rotation velocity in units

of km s^{-1} is plotted vs galactocentric radius R in kiloparsecs (kpc); 1 kpc \approx 3000 light years. It is seen that the RCs are flat to well beyond the edges of the optical disks (~ 10 kpc). Further Evidence for DM is provided by the Matter oscillation spectrum in galaxies, depicted in figure 6. The observed spectrum does not have the pronounced wiggles predicted by a baryon-only model, but it also has significantly higher power than does the model. In fact, $\Delta^2 = k^3 P(k)/(2\pi^2)$, which is a dimensionless measure of the clumping, never rises above one in a baryon-only model, so we could not see any large structures (clusters, galaxies, people, etc.) in the universe in such a model ²⁵.

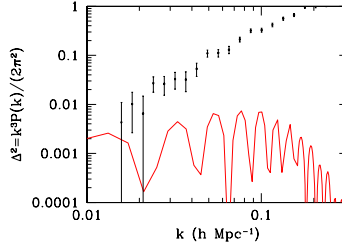


Figure 6. Power spectrum of matter fluctuations (red curve, with wiggles) in a theory without dark matter as compared to observations of the galaxy power spectrum.

However, at this stage we should mention the alternatives to Dark Matter models, the MOND ¹⁸, and its Lorentz-violating TeVeS field theory version ¹⁹, which could also reproduce the rotational curves of galaxies, by assuming modified Newtonian dynamics at galactic scales for small gravitational accelerations, smaller than a universal value $\gamma < \gamma_0 \sim (200\text{km sec}^{-1})^2/(10\text{kpc})$. MOND theories have been claimed to fit most of the rotational curves of galaxies (fig. 5), with few notable exceptions, though, e.g. the bullet cluster. It should be mentioned that TeVeS models, due to their preferred-cosmic-frame features, are characterized by “Aether”-Lorentz violating isotropic vector fields $A_\mu = (f(t), 0, 0, 0)$, $A_\mu A^\mu = -1$, whose cosmic instabilities are also claimed ²¹ to reproduce the enhanced growth of perturbations observed in galaxies (c.f. fig. 6). In these lectures I will not discuss such models. It should be noted at this point that such issues, namely whether there are dark matter particles or not, could be resolved in principle by particle physics searches at colliders or direct dark matter searches, which I will now come to.

3.2. Types of DM and Candidates

From nucleosynthesis constraints we can estimate today the baryonic energy density contribution to be of order: $\Omega_{baryons} = 0.045 \pm .01$, and this in fact is the dominant form of ordinary matter in the Universe. Thus, barring alternatives, 90% of the alleged matter content of the Universe seems to be dominated by DM of unknown composition at present. There are several dark matter candidates, which can be classified into two large categories depending on their origin and properties:

(I) Astrophysical: (i) MASSive Compact Halo ObectS (MACHOS): Dwarf stars and Planets (Baryonic Dark Matter) and Black Holes, (ii) Non-luminous Gas Clouds.

(II) Particles (Non-Baryonic Dark Matter): Weakly Interacting Massive Particles (WIMP), which might be the best candidates for DM: should not have electromagnetic or strong interactions. May have weak and gravitational interactions. WIMPS might include axions, neutrinos stable supersymmetric partners *etc.* If these WIMPS are thermal relics from the Big Bang then we can calculate their relic abundance today and compare with CMB and other astrophysical data. Non-thermal relics may also exist in some cosmological models but will not be the subject of our discussion in these lectures.

There is an alternative classification of DM, depending on the energetics of the constituting particles:

(i) Hot Dark Matter (HDM): form of dark matter which consists of particles that travel with ultra-relativistic velocities: e.g. neutrinos.

(ii) Cold Dark Matter (CDM): form of dark matter consisting of slowly moving particles, hence cold, e.g. WIMPS (stable supersymmetric particles (e.g. neutralinos *etc.*) or MACHOS.

(iii) Warm Dark Matter (WDM): form of dark matter with properties between those of HDM and CDM. Examples include sterile neutrinos, light gravitinos in supergravity theories *etc.*

Particle physics and/or astrophysics should provide candidates for DM and also explain the relic densities of the right order as that predicted by the data. Currently, the most favorite SUSY candidate for non baryonic CDM are neutralinos²⁶ $\tilde{\chi}$. These particles could be a WIMP if they are stable, which is the case in models where they are the Lightest SUSY Particles (LSP) (with typical masses $m_{\tilde{\chi}} > 35 \text{ GeV}$). Most of supersymmetric model constraints come from the requirement that a neutralino is the dominant astrophysical DM, whose relic abundance can explain the missing Universe

mass problem. I mention at this stage that direct searches for $\tilde{\chi}$ involve, among others, the recoil of nucleons during their interaction with $\tilde{\chi}$ in cryogenic materials. In these lectures we shall concentrate mainly on colliders DM searches. I refer the reader to ref. ²³ for direct DM searches and other pertinent terrestrial and extraterrestrial experiments.

3.3. WIMP DM: thermal properties and relic densities

In all the searches we shall deal with in the present work, which are also the most commonly studied in the literature, one makes the standard assumption that the dark matter particle, χ , is a *thermal relic* of the Big Bang: when the early Universe was dense and hot, with temperature $T \gg m_\chi$, χ was in *thermal equilibrium*; annihilation of χ and its antiparticle $\bar{\chi}$ into lighter particles, $\chi\bar{\chi} \rightarrow l\bar{l}$, and the inverse process $l\bar{l} \rightarrow \chi\bar{\chi}$ proceeded with equal rates ¹². As the Universe expanded and cooled down to a temperature $T < m_\chi$, the number density of χ dropped exponentially, $n_\chi \sim e^{-m_\chi/T}$. Eventually, the temperature became too low for the annihilation to keep up with the expansion rate and the species χ ‘froze out’ with the cosmological *abundance* (“relic”) observed today.

The time evolution of the number density $n_\chi(t)$ is determined by the Boltzmann equation ¹²,

$$dn_\chi/dt + 3Hn_\chi = -\langle\sigma_A v\rangle [(n_\chi)^2 - (n_\chi^{\text{eq}})^2], \quad (3.6)$$

where H is the Hubble expansion rate, n_χ^{eq} the equilibrium number density and $\langle\sigma_A v\rangle$ is the thermally averaged annihilation cross section summed over all contributing channels. It turns out that the relic abundance today is inversely proportional to the thermally averaged annihilation cross section, $\Omega_\chi h^2 \sim 1/\langle\sigma_A v\rangle$. The situation is depicted in fig. 7. When the properties and interactions of the WIMP are known, its thermal relic abundance can hence be computed from particle physics’ principles and compared with cosmological data.

3.4. Hot and Warm DM Excluded by WMAP

The WMAP/CMB results on the cosmological parameters discussed previously disfavor strongly Hot Dark Matter (neutrinos), as a result of the new determination of the upper bound on neutrino masses. The contribution of neutrinos to the energy density of the Universe depends upon the sum of the mass of the light neutrino species ^{12,6}:

$$\Omega_\nu h^2 = \frac{\sum_i m_i}{94.0 \text{ eV}} \quad (3.7)$$

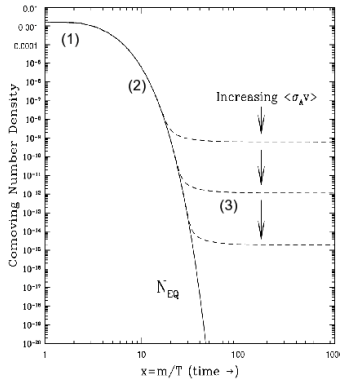


Figure 7. The full line is the equilibrium abundance; the dashed lines are the actual abundance after freeze-out. As the annihilation cross section $\langle\sigma_A v\rangle$ is increased, the WIMP stays in equilibrium longer, leading to a smaller relic density (from [12]).

where the sum includes neutrino species that are light enough to decouple while still relativistic.

The combined results from WMAP and other experiments⁶ on the cumulative likelihood of data as a function of the energy density in neutrinos lead to $\Omega_\nu h^2 < 0.0067$ (at 95% confidence limit). Adding the Lyman α data, the limit weakens slightly⁶: $\Omega_\nu h^2 < 0.0076$ or equivalently (from (3.7)): $\sum_i m_{\nu_i} < 0.69$ eV, where, we repeat again, the sum includes light species of neutrinos. This may then imply an average upper limit on electron neutrino mass $\langle m_\nu \rangle_e < 0.23$ eV. These upper bounds strongly disfavor Hot Dark Matter scenarios.

Caution should be exercised, however, when interpreting the above WMAP result. There is the underlying-theoretical-model dependence of these results, which stems from the assumption of an Einstein-FRW Cosmology, characterized by local Lorentz invariance. If Lorentz symmetry is violated, as, for instance, is the case of the TeVeS models alternative to DM, then neutrinos with (rest) masses of up to 2 eV could have an abundance of $\Omega_\nu \sim 0.15$ in order to reproduce the peaks in the observed CMB spectrum (fig. 3)²⁰ and thus being phenomenologically acceptable, at least from the CMB measurements viewpoint.

At this juncture we note that another important result of WMAP is the evidence for early re-ionization of the Universe at redshifts $z \simeq 20$. If one assumes that structure formation is responsible for re-ionization, then such early re-ionization periods are compatible only for high values of the

masses m_X of *Warm Dark Matter*. Specifically, one can exclude models with $m_X \leq 10$ KeV based on numerical simulations of structure formation for such models²⁷. Such simulations imply that dominant structure formation responsible for re-ionization, for Warm Dark Matter candidates with $m_X \leq 10$ KeV, occurs at much smaller z than those observed by WMAP. In view of this, one can therefore exclude popular particle physics models employing light gravitinos ($m_X \simeq 0.5$ KeV) as the Warm Dark Matter candidate. It should be noted at this stage that such structure formation arguments can only place a lower bound on the mass of the Warm Dark Matter candidate. The reader should bear in mind that Warm Dark Matter with masses $m_X \geq 100$ KeV becomes indistinguishable from Cold Dark Matter, as far as structure formation is concerned.

3.5. *Cold DM in Supersymmetric Models: Neutralino*

After the exclusion of Hot and Warm Dark Matter, the only type of Dark matter that remains consistent with the recent WMAP results⁶ is the *Cold Dark Matter*, which in general may consist of axions, superheavy particles (with masses $\sim 10^{14\pm 5}$ GeV)^{28,29} and stable supersymmetric partners. Indeed, one of the major and rather unexpected predictions of Supersymmetry (SUSY), broken at low energies $M_{SUSY} \approx \mathcal{O}(1 \text{ TeV})$, while R -parity is conserved, is the existence of a stable, neutral particle, the lightest neutralino ($\tilde{\chi}$), referred to as the lightest supersymmetric particle (LSP)²⁶. Such particle is an ideal candidate for the Cold Dark Matter in the Universe²⁶. Such a prediction fits well with the fact that SUSY is not only indispensable in constructing consistent string theories, but it also seems unavoidable at low energies ($\sim 1 \text{ TeV}$) if the gauge hierarchy problem is to be resolved. Such a resolution provides a measure of the SUSY breaking scale $M_{SUSY} \approx \mathcal{O}(1 \text{ TeV})$.

This type of Cold Dark Matter will be our focus from now on, in association with the recent results from WMAP3 on relic densities^{3,6}. The WMAP3 results, combined with other existing data, yield for the baryon and matter densities (including dark matter) at 2σ -level: $\Omega_m h^2 = 0.1268_{-0.0095}^{+0.0072}$ (matter), $100\Omega_b h^2 = 2.233_{-0.091}^{+0.072}$ (baryons). One assumes that CDM is given by the difference of these two. As mentioned already, in supersymmetric (SUSY) theories the favorite candidate for CDM is the lightest of the Neutralinos $\tilde{\chi}$ (SUSY CDM), which is stable, as being the Lightest SUSY particle (LSP) (There are cases where the stau or the sneutrino can be the lightest supersymmetric particles. These cases are not fa-

vored³⁰ and hence are not considered). From the WMAP3 results³, then, assuming $\Omega_{CDM} \simeq \Omega_\chi$, we can infer stringent limits for the neutralino χ relic density:

$$0.0950 < \Omega_\chi h^2 < 0.1117, \quad (3.8)$$

It is important to notice that in this inequality only the upper limit is *rigorous*. The lower Limit is *optional*, given that there might (and probably do) exist other contributions to the overall (dark) matter density. It is imperative to notice that all the constraints we shall discuss in this review are *highly model dependent*. The results on the minimal SUSY extensions of the standard model⁷, for instance, cannot apply to other models such as superstring-inspired ones, including non equilibrium cosmologies, which we shall also discuss here. However, formally at least, most of the analysis can be extrapolated to such models, with possibly different results, provided the SUSY dark matter in such models is thermal. Before moving into such a discussion we consider it as instructive to describe briefly various important properties of the Neutralino DM.

The Neutralino is a superposition of SUSY partner states. Its mass matrix in bino–wino–higgsinos basis $\psi_j^0 = (-i\lambda', -i\lambda^3, \psi_{H_1}^0, \psi_{H_2}^0)$ is given by

$$\mathcal{M}_N = \begin{pmatrix} M_1 & 0 & -m_{Zs_W}c_\beta & m_{Zs_W}s_\beta \\ 0 & M_2 & m_{Zc_W}c_\beta & -m_{Zc_W}s_\beta \\ -m_{Zs_W}c_\beta & m_{Zc_W}c_\beta & 0 & -\mu \\ m_{Zs_W}s_\beta & -m_{Zc_W}s_\beta & -\mu & 0 \end{pmatrix}$$

where M_1, M_2 : the U(1) and SU(2) gaugino masses, μ : higgsino mass parameter, $s_W = \sin \theta_W$, $c_W = \cos \theta_W$, $s_\beta = \sin \beta$, $c_\beta = \cos \beta$ and $\tan \beta = v_2/v_1$ ($v_{1,2}$ v.e.v. of Higgs fields $H_{1,2}$). The mass matrix is diagonalized by a unitary mixing matrix N , $N^* \mathcal{M}_N N^\dagger = \text{diag}(m_{\tilde{\chi}_1^0}, m_{\tilde{\chi}_2^0}, m_{\tilde{\chi}_3^0}, m_{\tilde{\chi}_4^0})$, where $m_{\tilde{\chi}_i^0}$, $i = 1, \dots, 4$, are the (non-negative) masses of the physical neutralino states with $m_{\tilde{\chi}_1^0} < \dots < m_{\tilde{\chi}_4^0}$. The lightest neutralino is then:

$$\tilde{\chi}_1^0 = N_{11}\tilde{B} + N_{12}\tilde{W} + N_{13}\tilde{H}_1 + N_{14}\tilde{H}_2.$$

To calculate relic densities it is assumed that the initial number density of neutralinos χ particle in the Early Universe has been in thermal equilibrium: interactions creating χ usually happen as frequently as the reverse interactions which destroy them. Eventually the temperature of the expanding Universe drops to the order of the neutralino (rest) mass $T \simeq m_\chi$. In such a situation, most particles no longer have sufficient energy to create

neutralinos. Now neutralinos can only *annihilate*, until their rate becomes smaller than the Hubble expansion rate, $H \geq \Gamma_{\text{ann}}$. Then, Neutralinos are being separated apart from each other too quickly to maintain equilibrium, and thus they reach their freeze-out temperature, $T_F \simeq m_\chi/20$, which characterizes this type of cold dark matter.

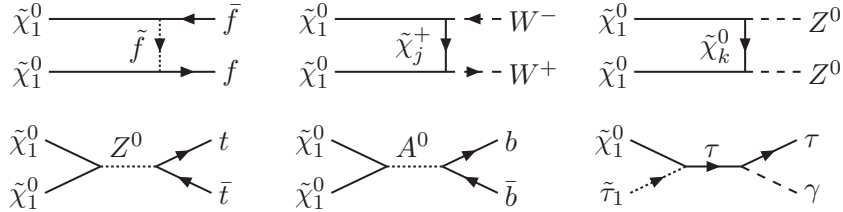


Figure 8. Basic Neutralino annihilations including stau co-annihilations in MSSM (from S. Kraml, *Pramana* 67, 597 (2006) [hep-ph/0607270]).

In most neutralino relic density calculations, the only interaction cross sections that need to be calculated are annihilations of the type $\chi\chi \rightarrow X$ where χ is the lightest neutralino and X is any final state involving only Standard Model particles. However, there are scenarios in which other particles in the thermal bath have important effects on the evolution of the neutralino relic density. Such a particle annihilates with the neutralino into Standard Model particles and is called a *co-annihilator* (c.f. figure 8). In order for a particle to be an *Effective co-annihilator*, it must have direct interactions with the neutralino and must be *nearly degenerate* in mass: Such degeneracy happens in the Minimal Supersymmetric Standard Model (MSSM), for instance, with possible co-annihilators being the lightest stau, the lightest stop, the second-to-lightest neutralino or the lightest chargino. When this degeneracy occurs, the neutralino and all relevant co-annihilators form a coupled system.

Without co-annihilations the evolution of a relic particle number density, n , is governed, as mentioned previously, by a single-species Boltzmann equation (3.6). It should be noted that the relic-particle number density is modified by the Hubble expansion and by direct and inverse annihilations of the relic particle. The Relic particle is assumed stable, so relic decay is neglected. Also commonly assumed is time-reversal (T) invariance, which relates annihilation and inverse annihilation processes. In the presence of co-annihilators the Boltzmann equation gets more complicated but it can

be simplified using stability properties of relic particle and co-annihilators (using $n = \sum_{i=1}^N n_i$):

$$\frac{dn}{dt} = -3Hn - \sum_{i,j=1}^N \langle \sigma_{ij} v_{ij} \rangle (n_i n_j - n_i^{\text{eq}} n_j^{\text{eq}}) . \quad (3.9)$$

To a very good approximation, one can use an effective single species Boltzmann equation for this case if $\langle \sigma v \rangle = \sum_{i,j} \langle \sigma_{ij} v_{ij} \rangle \frac{n_i^{\text{eq}} n_j^{\text{eq}}}{n^{\text{eq}} n^{\text{eq}}}$.

The Boltzmann equation (3.9) can be solved numerically, but in most cases even analytically. Details on how to solve the Boltzmann equation are given abundantly in the cosmology literature¹² and will not be repeated here. We shall only outline the most important results that will be essential for our discussion in these lectures. One should determine the freeze-out temperature $x_F = m_\chi/T_F$: $x_F = \ln \left(\frac{0.038 g m_{\text{pl}} m_\chi \langle \sigma v \rangle}{\sqrt{g_*} x_F} \right)$, with m_{pl} the Planck mass, g the total number of degrees of freedom of the χ particle (spin, color, etc.), g_* the total number of effective relativistic degrees of freedom at freeze-out, and the thermally averaged cross section is evaluated at the freeze-out temperature. For most CDM candidates, $x_F \simeq 20$. The total (co)annihilation depletion of neutralino number density is calculated by integrating the thermally averaged cross section from freeze-out to the present temperature:

$$\Omega_\chi h^2 = 40 \sqrt{\frac{\pi}{5}} \frac{h^2 s_0}{H_0^2 m_{\text{Pl}}^3} \frac{1}{(g_{*S}/g_*^{1/2}) J(x_F)} = \frac{1.07 \times 10^9 \text{ GeV}^{-1}}{g_*^{1/2} m_{\text{pl}} J(x_F)} ,$$

$$J(x_F) = \int_{x_F}^{\infty} \langle \sigma v \rangle x^{-2} dx . \quad (3.10)$$

where s_0 is the entropy density, g_{*S} denotes the number of effective relativistic d.o.f. contributing to the (constant) entropy of the universe and h is the reduced Hubble parameter: $H_0 = 100 h \text{ km sec}^{-1} \text{ Mpc}^{-1}$. This is the expression one compares with the experimental determination of the DM abundance via, e.g., WMAP data. It should be noted at this stage that the theoretical assumptions leading to the above results may not hold in general for all DM models and candidates: the missing non-baryonic matter in the universe may only partially, or not at all, consist of relic neutralinos. Also, as we shall discuss later on the article, in some off-shell, non-equilibrium relaxation stringy models of dark energy, the Boltzmann equation gets modified by off-shell, non-equilibrium terms as well as time-dependent dilaton-source terms. This leads to important modifications on the associated particle-physics models constraints.

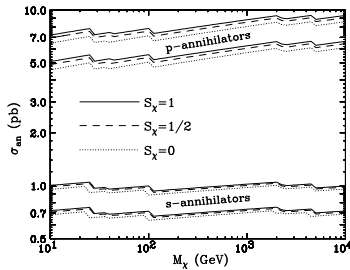


Figure 9. Values of the quantity σ_{an} allowed at 2σ level as a function of the DM mass.

3.6. Model-Independent DM Searches in Colliders

As we have discussed above, if dark matter comes from a thermal relic, its density is determined, to a large extent, by the dark matter annihilation cross section: $\sigma(\chi\chi \rightarrow SM SM)$. Indeed, as already mentioned, the present-day dark matter abundance is roughly inversely proportional to the thermally averaged annihilation cross section times velocity, $\Omega_\chi h^2 \propto 1/\langle\sigma v\rangle$. This latter quantity can be conveniently expanded in powers of the relative dark matter particle velocity:

$$\sigma v = \sum_J \sigma_{an}^{(J)} v^{(2J)}. \quad (3.11)$$

Usually, only the lowest order non-negligible power of v dominates. For $J = 0$, such dark matter particles are called s -annihilators, and for $J = 1$, they are called p -annihilators; powers of J larger than 1 are rarely needed.:

Figure 9 shows the constraint on the annihilation cross section as a function of dark matter mass that results from Eq. (3.8)³¹. The lower (upper) band of fig. 9 is for models where s -wave (p -wave) annihilation dominates. It is important to notice³¹ that the total annihilation cross section σ_{an} is virtually insensitive to dark-matter mass. This latter effect is due to the changing number of degrees of freedom at the time of freeze-out as the dark matter mass changes. It also points to cross sections expected from weak-scale interactions (around $0.8 pb$ for s -annihilators and $6 pb$ for p -annihilators), hence implying the possibility that DM is connected to an explanation for the weak scale and thus WIMPs³¹. Such WIMPs exist not only in supersymmetric theories, of course, but in a plethora of other models such as theories involving extra dimensions and 'little Higgs' models. The LHC and the ILC are specifically designed to probe the origin of the weak scale, so dark matter searches and future collider physics ap-

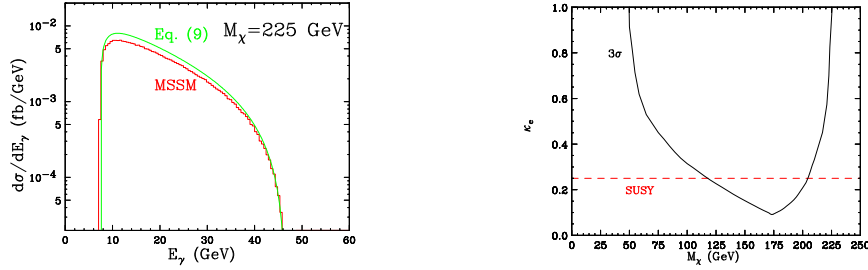


Figure 10. *Left panel:* Comparison between the photon spectra from the process $e^+e^- \rightarrow 2\chi_1^0 + \gamma$ in the explicit supersymmetric models defined in A. Birkedal, K. Matchev and M. Perelstein, Phys. Rev. D **70**, 077701 (2004) (red/dark-gray) and the predicted spectra for a p -annihilator of the corresponding mass and κ_e (green/light-gray). *Right panel:* The reach of a 500 GeV unpolarized electron-positron collider with an integrated luminosity of 500 fb^{-1} for the discovery of p -annihilator WIMPs, as a function of the WIMP mass M_χ and the e^+e^- annihilation fraction κ_e . The 3σ (black) contour is shown, along with an indication of values one might expect from supersymmetric models (red dashed line, labelled 'SUSY'). Only statistical uncertainty is included.

pear to be closely related. The next question one could ask is whether the above cross section could be turned, within a WIMP working hypothesis framework, into a model-independent signature at colliders. This question was answered in the affirmative in ³¹. One introduces the parameter $\kappa_e \equiv \sigma(\chi\chi \rightarrow e^+e^-)/\sigma(\chi\chi \rightarrow SM|SM)$ which relates dark matter annihilation processes to cross sections involving e^+e^- in the final state. Using crossing symmetries to relate $\sigma(\chi\chi \rightarrow e^+e^-)$ to $\sigma(e^+e^- \rightarrow \chi\chi)$ and collinear factorization one can relate $\sigma(e^+e^- \rightarrow \chi\chi)$ to $\sigma(e^+e^- \rightarrow \chi\chi\gamma)$, thus connecting astrophysical data on σ_{an} to the process $e^+e^- \rightarrow \chi\chi\gamma$. The resulting differential cross section reads ³¹

$$\frac{d\sigma}{dx d\cos\theta}(e^+e^- \rightarrow 2\chi + \gamma) \simeq \frac{\alpha \kappa_e \sigma_{\text{an}}}{16\pi} \frac{1 + (1-x)^2}{x} \frac{1}{\sin^2\theta} 2^{J_0} (2S_\chi + 1)^2 \left(1 - \frac{4M_\chi^2}{(1-x)s}\right)^{\frac{1}{2} + J_0} \quad (3.12)$$

with α the appropriate fine structure constant, $x = 2E_\gamma/\sqrt{s}$, θ angle between photon and incoming electron, S_χ spin of WIMP, J_0 is the dominant value of J in the velocity expansion of (3.11) (as discussed above, commonly $J = 0$ dominates, s -annihilator DM). The accuracy of the method and its predictions are illustrated in fig. 10, where the left panel illustrates the results obtained using the formula (3.12), which are then compared with those of an exact calculation, based on a supersymmetric MSSM model,

with WIMP masses 225 GeV, whilst the right panel shows the expected reach in κ_e for a 500 GeV linear e^+e^- collider as a function of the WIMP mass. As we observe from such comparisons the results of the method and of the exact calculation are in pretty good agreement.

We note at this stage, however, that, although model independent, the above process is rarely the dominant collider signature of new physics within a given model. It therefore makes sense to look for model dependent processes at colliders, which we now turn to. In this last respect, it is important to realize ³¹ that a calculation of slepton masses is essential for computing accurately relic abundances in theoretical models; without a collider measurement of the slepton mass, there may be a significant uncertainty in the relic abundance calculation. This uncertainty results because the slepton mass should then be allowed to vary within the whole experimentally allowed range. We mention here that measuring slepton masses at LHC is challenging due to W^+W^- and $t\bar{t}$ production. However, as shown in ³¹, it is possible through the study of di-lepton mass distribution $m_{\ell\ell}$ in the decay channel $\tilde{\chi}_2^0 \rightarrow \ell^\pm \ell^\mp \tilde{\chi}_1^0$ and also at the International Linear Collider (ILC). The reader is referred to the literature ³¹ for further details on these important issues. We are now ready to start our discussion on model-dependent DM signatures at LHC and future colliders.

4. Model-Dependent WMAP SUSY Constraints

We shall concentrate on DM signatures at colliders, using WMAP1,3 data. To illustrate the underlying-theoretical-model dependence of the results we chose three representative theoretical models: (i) the mSUGRA (or constrained MSSM model) ^{8,7}, (ii) a heterotic string model with orbifold compactification ⁹, and (iii) a non-critical (non-equilibrium) stringy cosmology (Q-cosmology) with running dilatons (implying a dilaton quintessence relaxation model for dark energy at late eras) and off-shell terms ¹⁰.

4.1. Constrained MSSM/mSUGRA Model

MSSM has too many parameters to be constrained effectively by data. To minimize the number of parameters one can “embed” this model by taking into account the gravity sector, which from a cosmological point of view is a physical necessity. Such an embedding in principle affects the dark energy sector of the cosmology, and in fact the minimal Supergravity model (mSUGRA) ⁸, used to yield the Constrained MSSM (CMSSM) predicts too large values of the cosmological constant at a quantum level, and hence it

should not be viewed as the physical model. Nevertheless, as far as DM searches are concerned, such models give a pretty good idea of how astrophysical data can be used to constrain particle physics models, and this is the point of view we take in this work. mSUGRA is the best studied model so far as far as constraints on supersymmetric models using astrophysical CMB data are concerned. A relatively recent review on such approaches is given in ⁷, where we refer the reader for details and further material and references. In our presentation here we shall be very brief and concentrate only on the basic conclusions of such analyses.

4.1.1. *Basic Features: geometry of the parameter space*

Before embarking into a detailed analysis of the constraints of the minimal supersymmetric standard model embedded in a minimal supergravity model (CMSSM) ⁸, we consider it useful to outline the basic features of these models, which will be used in this review. The embedding of SUSY models into the minimal supergravity (mSUGRA) model implies that there are five independent parameters: Three of them, the scalar and gaugino masses $m_0, m_{1/2}$ as well as the trilinear soft coupling A_0 , at the unification scale, set the size of the Supersymmetry breaking scale. In addition one can consider as input parameter $\tan\beta = \frac{\langle H_2 \rangle}{\langle H_1 \rangle}$, the ratio of the v.e.v's of the Higgses H_2 and H_1 giving masses to up and down quarks respectively. The sign (signature) of the Higgsino mixing parameter μ is also an input but not its size which is determined from the Higgs potential minimization condition ⁷. The parameter space of mSUGRA can be effectively described in terms of two branches:

(i) An Ellipsoidal Branch (EB) of Radiative Symmetry Breaking, which exists for small to moderate values of $\tan\beta \lesssim 7$, where the loop corrections are typically small. One finds that the radiative symmetry breaking constraint demands that the allowed set of soft parameters m_0 and a combination ⁷ $m'_{12} = f(m_{1/2}, A_0, \tan\beta)$ lie, for a given value of μ , on the surface of an *Ellipsoid*. This places upper bounds on the sparticle masses for a given value of $\Phi \equiv \mu^2/M_Z^2 + 1/4$.

(ii) Hyperbolic Branch (HB) of Radiative Symmetry Breaking. This branch is realized ³² for large values of $\tan\beta \gtrsim 7$, where the loop corrections to μ are significant. In this branch, $(m_0, m'_{1/2})$ lie now on the surface of a *hyperboloid*: $\frac{m'_{1/2}{}^2}{\alpha^2(Q_0)} - \frac{m_0^2}{\beta^2(Q_0)} \simeq \pm 1$, $Q_0 = 0$ a fixed value of the running scale, α, β constant functions of Φ, M_Z, A_0 . For fixed A_0 , the $m_0, m_{1/2}$ lie on a *hyperbola*, hence they can get large for fixed μ or Φ . What

is interesting in the HB case is the fact that m_0 and/or $m_{1/2}$ can become very large, while much smaller values for μ can occur.

(ia) A subset of HB is the so-called *high zone*³². In this case electroweak symmetry breaking (EWSB) can occur in regions where m_0 and $m_{1/2}$ can be in the several TeV range, with much smaller values for the parameter μ which however is much larger than M_Z . This has important consequences for phenomenology, as we shall see. In this zone the lightest of the neutralinos, χ_1 , is almost a Higgsino having a mass of order μ . This is called *inversion phenomenon* since the LSP is a Higgsino rather a Bino. The inversion phenomenon has dramatic effects on the nature of the particle spectrum and SUSY phenomenology in this HB. Indeed, as we discussed above, in mSUGRA one naturally has co-annihilation with the sleptons when the neutralino mass extends to masses beyond 150-200 GeV with processes of the type (c.f. fig. 8): $\chi\tilde{\ell}_R^a \rightarrow \ell^a\gamma, \ell^a Z, \ell^a h$, $\tilde{\ell}_R^a\tilde{\ell}_R^b \rightarrow \ell^a\ell^b$, and $\tilde{\ell}_R^a\tilde{\ell}_R^{b*} \rightarrow \ell^a\bar{\ell}^b, \gamma\gamma, \gamma Z, ZZ, W^+W^-, hh$, where $\tilde{\ell}$ is essentially a $\tilde{\tau}$. Remarkably the relic density constraints can be satisfied on the hyperbolic branch also by co-annihilation. However, on the HB the co-annihilation is of an entirely different nature as compared with the stau co-annihilations discussed previously: instead of a neutralino-stau co-annihilation, and stau - stau in the HB one has co-annihilation processes involving the second lightest neutralino and chargino states³³, $\chi_1^0 - \chi_1^\pm$, followed by $\chi_1^0 - \chi_2^0, \chi_1^+ - \chi_1^-, \chi_1^\pm - \chi_2^0$. Some of the dominant processes that contribute to the above co-annihilation processes are³³: $\chi_1^0\chi_1^+, \chi_2^0\chi_1^+ \rightarrow u_i\bar{d}_i, \bar{e}_i\nu_i, AW^+, ZW^+, W^+h$ and $\chi_1^+\chi_1^-, \chi_1^0\chi_2^0 \rightarrow u_i\bar{u}_i, d_i\bar{d}_i, W^+W^-$. Since the mass difference between the states χ_1^+ and χ_1^0 is the smallest the $\chi_1^0\chi_1^+$ co-annihilation dominates. In such cases, the masses m_0 $m_{1/2}$ may be pushed beyond 10 TeV, so that squarks and sleptons can get masses up to several TeV, i.e. beyond detectability limits of immediate future accelerators such as LHC.

(ib) Except the high zone where the inversion phenomenon takes place the HB includes the so called *Focus Point* (FP) region³⁴, which is defined as a region in which some renormalization group (RG) trajectories intersect (FP region would be only a point, were it not for threshold effects which smear it out). We stress that the FP is *not* a fixed point of the RG. The FP region is a subset of the HB limited to relatively low values of $m_{1/2}$ and values of μ close to the electroweak scale, M_Z , while m_0 can be a few TeV but not as large as in the high zone due to the constraints imposed by the EWSB condition. The LSP neutralino in this region is a mixture of Bino and Higgsino and the Higgsino impurity allows for rapid

s-channel LSP annihilations, resulting to low neutralino relic densities at experimentally acceptable levels. This region is characterized by m_0 in the few TeV range, low values of $m_{1/2} \ll m_0$ and rather small values of μ close to M_Z . The LSP neutralino in this case is a mixture of Bino and Higgsino and its Higgsino impurity is adequate to give rise to rapid s-channel LSP annihilations so that the neutralino relic density is kept low at experimentally acceptable values. Since μ is small the lightest chargino may be lighter than 500 GeV and the FP region may be accessible to future TeV scale colliders. Also due to the relative smallness of $m_{1/2}$ in this region gluino pair production may occur at a high rate making the FP region accessible at LHC energies.

It should be pointed out that, although the HB may be viewed as fine tuned, nevertheless recent studies³⁵, based on a χ^2 analysis, have indicated that the WMAP data, when combined with data on $b \rightarrow s\gamma$ and $g_\mu - 2$, seem to favor the Focus Point HB region and the large $\tan \beta$ neutralino resonance annihilation of mSUGRA.

4.1.2. Muon's anomaly and SUSY detection prospects

Undoubtedly one of the most significant experimental results of the last years is the measurement of the anomalous magnetic moment of the muon³⁶. Deviation of its measured value from the Standard Model (SM) predictions is evidence for new physics with Supersymmetry being the prominent candidate to play that role. Adopting Supersymmetry as the most natural extension of the SM, such deviations may be explained and impose at the same time severe constraints on the predictions of the available SUSY models by putting upper bounds on sparticle masses. Therefore knowledge of the value of $g_\mu - 2$ is of paramount importance for Supersymmetry and in particular for the fate of models including heavy sparticles in their mass spectrum, as for instance those belonging to the Hyperbolic Branch.

Unfortunately the situation concerning the anomalous magnetic moment is not clear as some theoretical uncertainties remain unsettled as yet. Until last year, as far as I am aware of, there were two theoretical estimates for the difference of the experimentally measured³⁶ value of $a_\mu = (g_\mu - 2)/2$ from the theoretically calculated one within the SM³⁷,

- Estimate (I) $a_\mu^{\text{exp}} - a_\mu^{\text{SM}} = 1.7(14.2) \times 10^{-10}$ $[0.4(15.5) \times 10^{-10}]$
- Estimate (II) $a_\mu^{\text{exp}} - a_\mu^{\text{SM}} = 24.1(14.0) \times 10^{-10}$ $[22.8(15.3) \times 10^{-10}]$

In (I) the τ -decay data are used in conjunction with Current Algebra while in (II) the $e^-e^+ \rightarrow \text{Hadrons}$ data are used in order to extract the photon vacuum polarization which enters into the calculation of $g_\mu - 2$. Within square brackets are updated values of Ref. ³⁷ ¹. Estimate (I) is considered less reliable since it carries additional systematic uncertainties and for this reason in many studies only the Estimate (II) is adopted. Estimate (II) includes the contributions of additional scalar mesons not taken into account in previous calculations.

In order to get an idea of how important the data on the muon anomaly might be we quote Ref. ³² where both estimates have been used. If Estimate (II) is used at a 1.5σ range much of the HB and all of the inversion region can be eliminated. In that case the usually explored region of SUSY in the EB is the only one that survives, which, as we shall discuss below, can be severely constrained by means of the recent WMAP data. On the other hand, Estimate (I), essentially implies no difference from the SM value, and hence, if adopted, leaves the HB, and hence its high zone (inversion region), *intact*. In such a case, SUSY may not be detectable at colliders, at least in the context of the mSUGRA model, but may be detectable in some direct dark matter searches, to which we shall turn to later in the article.

For the above reasons, it is therefore *imperative* to determine unambiguously the muon anomalous magnetic moment $g_\mu - 2$ by reducing the errors in the leading order hadronic contribution, experimentally, and improving the theoretical computations within the standard model. In view of its importance for SUSY searches, it should also be necessary to have further experiments in the future, that could provide independent checks of the measured muon magnetic moment by the E821 experiment ³⁶. Quite recently (2006) a new measurement ¹¹ of the $g_\mu - 2$ became available, which shows a clear discrepancy from the theoretically calculated Standard Model prediction by 3.4σ

$$1.91 \times 10^{-9} < \Delta a_\mu < 3.59 \times 10^{-9} \quad (4.13)$$

thereby pointing towards the elimination of the inversion region of the HB of mSUGRA, according to the above discussion.

¹Due to the rapid updates concerning $g_\mu - 2$ the values of $a_\mu^{\text{exp}} - a_\mu^{\text{SM}}$ used in previous works quoted in this article may differ from those appearing above.

4.1.3. WMAP $mSUGRA$ Constraints in the EB

After the first year of running of WMAP, there have been two independent groups working on this update of the CMSSM in light of the WMAP data, with similar results ^{38,39} and below we summarize the results of ³⁸ in fig. 11 for some typical values of the parameters $\tan\beta$ and signature of μ . In such analyses one plots m_0 vs. $m_{1/2}$, taking into account the calculated relic abundance of neutralinos in the model and constraining it by means of the WMAP results (3.8). Details are given in ⁷ and references therein.

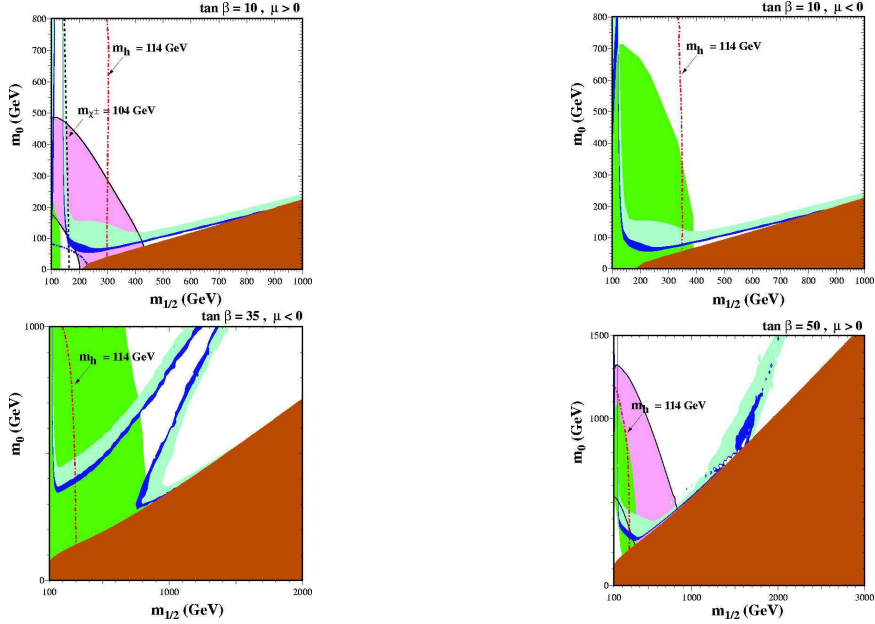


Figure 11. $mSUGRA/CMSSM$ constraints after WMAP from Ref. [38]. The Dark Blue shaded region is favored by WMAP1 ($0.094 \leq \Omega_\chi h^2 \leq 0.129$). Turquoise shaded regions have $0.1 \leq \Omega_\chi h^2 \leq 0.3$. Brick red shaded regions are excluded because LSP is charged. Dark green regions are excluded by $b \rightarrow s\gamma$. The Pink shaded region includes $2 - \sigma$ effects of $g_\mu - 2$. Finally, the dash-dotted line represents the LEP constraint on \tilde{e} mass.

For the LSP, the lightest of the charginos, stops, staus and Higgses the upper bounds on their masses of order of a few hundreds of GeV ⁷, for various values of the parameter $\tan\beta$, if the new WMAP determination ^{3,6} of the Cold Dark Matter (3.8) and the 2σ bound $149 < 10^{-11} \alpha_\mu^{SUSY} < 573$ of E821 is respected. The lightest of the charginos has a mass whose

upper bound is ≈ 550 GeV, and this is smaller than the upper bounds put on the masses of the lightest of the other charged sparticles, namely the stau and stop. Hence the prospects of discovering CMSSM at a e^+e^- collider with center of mass energy $\sqrt{s} = 800$ GeV, are *not* guaranteed. Thus, a center of mass energy of at least $\sqrt{s} \approx 1.1$ TeV is required to discover SUSY through chargino pair production. Note that in the allowed regions the next to the lightest neutralino, $\tilde{\chi}'$, has a mass very close to the lightest of the charginos and hence the process $e^+e^- \rightarrow \tilde{\chi}\tilde{\chi}'$, with $\tilde{\chi}'$ subsequently decaying to $\tilde{\chi} + l^+l^-$ or $\tilde{\chi} + 2$ jets, is kinematically allowed for such large $\tan\beta$, provided the energy is increased to at least $\sqrt{s} = 860$ GeV. It should be noted however that this channel proceeds via the t -channel exchange of a selectron and it is suppressed due to the heaviness of the exchanged sfermion. Therefore only if the center of mass energy is increased to $\sqrt{s} = 1.1$ TeV supersymmetry can be discovered in a e^+e^- collider provided it is based on the Constrained scenario ³⁹.

An important conclusion, therefore, which can be inferred by inspecting the figures 11 is that the constraints implied by a possible discrepancy of $g_\mu - 2$ from the SM value, as seems to be supported by the 2006 data ¹¹ (4.13), ($\alpha_\mu^{SUSY} \gtrsim 15.0 \times 10^{-10}$), when combined with the WMAP restrictions on CDM (neutralino) relic densities (3.8), imply severe restrictions on the available parameter space of the EB and lower significantly the upper bounds on the allowed neutralino masses $m_{\tilde{\chi}}$.

4.1.4. WMAP *mSUGRA* Constraints in the HB

Despite the above-mentioned good prospects of discovering minimal SUSY models at future colliders, if the EB is realized, however, things may not be that simple in Nature. χ^2 studies ³⁵ of *mSUGRA* in light of the recent WMAP data has indicated (c.f. figure 12) that the HB/focus point region of the model's parameter space seems to be favored along with the neutralino resonance annihilation region for $\mu > 0$ and large $\tan\beta$ values. The favored focus point region corresponds to moderate to large values of the Higgs parameter μ^2 , and large scalar masses m_0 in the several TeV range. The situation in case the HB is included in the analysis is depicted in figure 13 ³², where we plot the $m_0 - m_{1/2}$ graphs, as well as graphs of $m_0, m_{1/2}$ vs the neutralino LSP mass. The neutralino density is that of the WMAP data.

We stress again that, in case the high zone (inversion) region of the HB is realized, then the detection prospects of SUSY at LHC are diminished

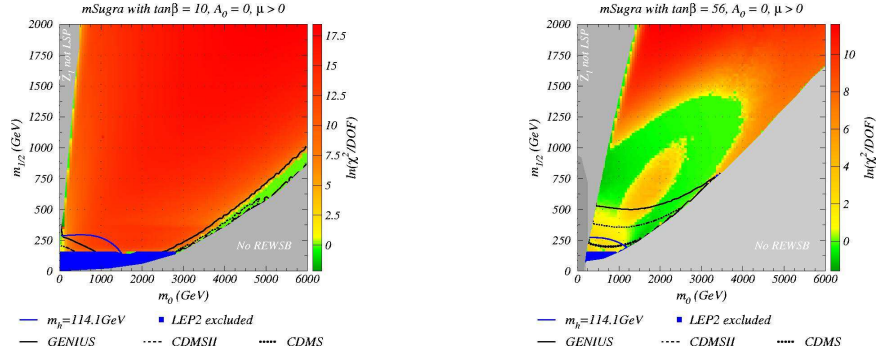


Figure 12. WMAP data seem to favor ($\frac{\chi^2}{dof} < 4/3$) (green) the HB/focus point region (moderate to large values of μ , large m_0 scalar masses) for almost all $\tan\beta$ (Left), as well as s - channel Higgs resonance annihilation (Right) for $\mu > 0$ and large $\tan\beta$.

significantly, in view of the fact that in such regions slepton masses may lie in the several TeV range (see figure 13). Fortunately, as already mentioned, last year's $g_\mu - 2$ data¹¹ (4.13) seem to exclude this possibility.

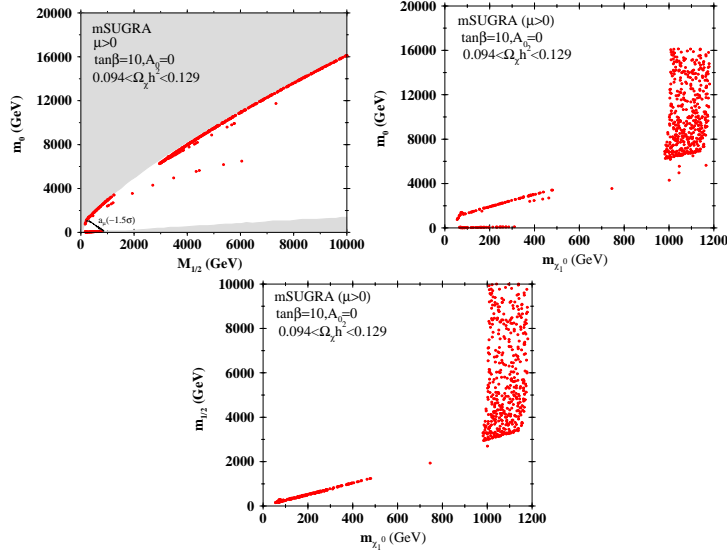


Figure 13. $m_0 - m_{1/2}$ graph, and m_0 and $m_{1/2}$ vs. m_χ graphs, including the HB of $mSUGRA$. Such regions are favored by the WMAP data.

4.1.5. Expected Reach of LHC and Tevatron

In view of the above results, an updated reach of LHC in view of the recent WMAP and other constraints discussed above (see figure 14) has been performed in ⁴⁰, showing that a major part of the HB, but certainly not its high zone (which though seems to be excluded by means of the recent $g_\mu - 2$ data (4.13)), can be accessible at LHC. The conclusion from this study ⁴⁰

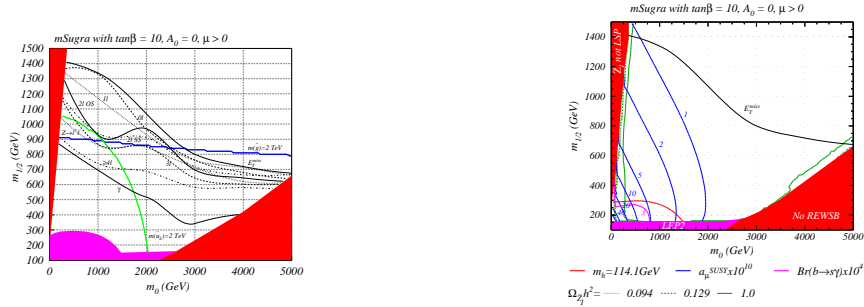


Figure 14. *Left:* The updated Reach in $(m_0, m_{1/2})$ parameter plane of mSUGRA assuming 100 fb^{-1} integrated luminosity. Red (magenta) regions are excluded by theoretical (experimental) constraints. *Right:* Contours (in view of the uncertainties) of several low energy observables : CDM relic density (green), contour of $m_h = 114.1 \text{ GeV}$ (red), contours of $a_\mu 10^{10}$ (blue) and contours of $b \rightarrow s\gamma \text{ BF} (\times 10^4)$ (magenta).

is that for an integrated luminosity of 100 fb^{-1} values of $m_{1/2} \sim 1400 \text{ GeV}$ can be probed for small scalar masses m_0 , corresponding to gluino masses $m_{\tilde{g}} \sim 3 \text{ TeV}$. For large m_0 , in the hyperbolic branch/focus point region, $m_{1/2} \sim 700 \text{ GeV}$ can be probed, corresponding to $m_{\tilde{g}} \sim 1800 \text{ GeV}$. It is also concluded that the LHC (CERN) can probe the entire stau co-annihilation region and most of the heavy Higgs annihilation funnel allowed by WMAP data, except for some range of $m_0, m_{1/2}$ in the case $\tan\beta \gtrsim 50$. A similar updated reach study in light of the new WMAP data has also been done for the Tevatron ⁴¹, extending previous analyses to large m_0 masses up to 3.5 TeV , in order to probe the HB/focus region favored by the WMAP data ³⁵. Such studies (c.f. figure 15) indicate that for a 5σ (3σ) signal with 10 (25) fb^{-1} of integrated luminosity, the Tevatron reach in the trilepton channel extends up to $m_{1/2} \sim 190$ (270) GeV independent of $\tan\beta$, which corresponds to a reach in terms of gluino mass of $m_{\tilde{g}} \sim 575$ (750) GeV .

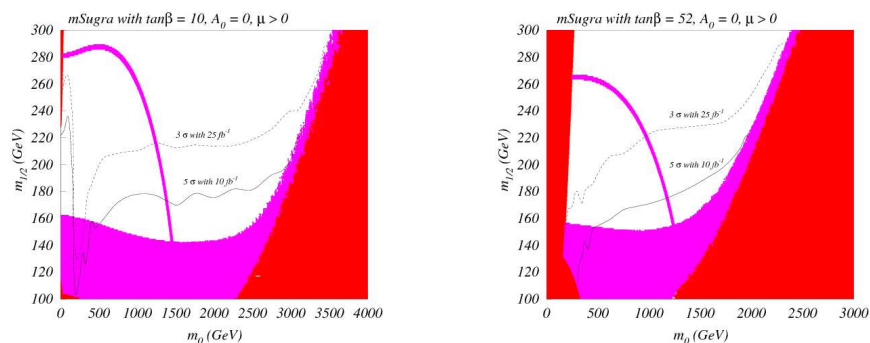


Figure 15. Left: The reach of Fermilab Tevatron in the m_0 vs. $m_{1/2}$ parameter plane of the mSUGRA model, with $\tan\beta = 10$, $A_0 = 0$ and $\mu > 0$, assuming a 5σ signal at 10 fb^{-1} (solid) and a 3σ signal with 25 fb^{-1} of integrated luminosity (dashed). The red (magenta) region is excluded by theoretical (experimental) constraints. The region below the magenta contour has $m_h < 114.1 \text{ GeV}$, in violation of Higgs mass limits from LEP2. Right: The reach of Fermilab Tevatron in the m_0 vs. $m_{1/2}$ parameter plane of the mSUGRA model, with $\tan\beta = 52$, $A_0 = 0$ and $\mu > 0$. The red (magenta) region is excluded by theoretical (experimental) constraints. The region below the magenta contour has $m_h < 114.1 \text{ GeV}$, in violation of Higgs mass limits from LEP2.

4.1.6. Astrophysical and Collider Dark Matter

Above we have analyzed constraints placed on supersymmetric particle physics models, in particular MSSM, by WMAP/CMB astrophysical data. The analysis made the assumption that neutralinos constitute exclusively the astrophysical DM. It would be desirable to inverse the logic and ask the question ⁴²: “are neutralinos produced at the LHC the particles making up the astronomically observed dark matter?”

To answer this question, let us first recall the relevant neutralino interactions (within the mSUGRA framework) that could take place in the Early universe (fig. 16). As we have discussed previously, the WMAP3

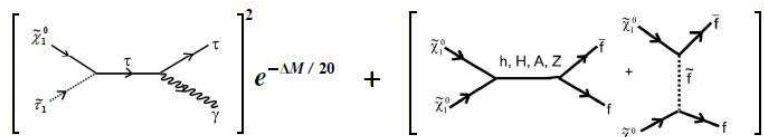


Figure 16. The Feynman diagrams for annihilation of neutralino dark matter in the early universe. The Boltzmann factor $e^{-\Delta M/20}$ in the tau-co-annihilation graph is explicitly indicated.

constraint (3.8) limits the parameter space to three main regions arising from the above diagrams (there is also a small “bulk” region): (1) The stau-neutralino ($\tilde{\tau}_1 - \tilde{\chi}_1^0$) co-annihilation region. Here m_0 is small and $m_{1/2} \leq 1.5$ TeV. (2) The focus region where the neutralino has a large Higgsino component. Here $m_{1/2}$ is small and $m_0 \geq 1$ TeV. (3) The funnel region where annihilation proceeds through heavy Higgs bosons which have become relatively light. Here both m_0 and $m_{1/2}$ are large. A key element in the co-annihilation region is the Boltzmann factor from the annihilation in the early universe at $kT \sim 20$ GeV: $\exp[-\Delta M/20]$, $\Delta M = M_{\tilde{\tau}_1} - M_{\tilde{\chi}_1^0}$ implying that significant co-annihilation occurs provided $\Delta M \leq 20$ GeV.

The accelerator constraints further restrict the parameter space and if the muon $g_\mu - 2$ anomaly maintains ¹¹, (c.f. (4.13)), then $\mu > 0$ is preferred and there remains mainly the co-annihilation region (c.f. figure 17). Note

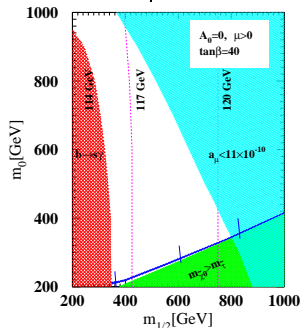


Figure 17. Allowed parameter space in mSUGRA. Dashed vertical lines are possible Higgs masses (from [42]).

the cosmologically allowed narrow co-annihilation band, due to the Boltzmann factor for $\Delta M = 5 - 15$ GeV, corresponding to the allowed WMAP range for $\Omega_{\tilde{\chi}_1^0} h^2$.

One may ask, then, whether: (i) such a small stau-neutralino mass difference (5-15 GeV) arise in mSUGRA, since one would naturally expect these SUSY particles to be hundreds of GeV apart and (ii) such a small mass difference be measured at the LHC. If the answer to both these questions is in the affirmative, then the observation of such a small mass difference would be a strong indication ⁴² that the neutralino is the astronomical DM particle, since it is the cosmological constraint on the amount of DM that forces the near mass degeneracy with the stau, and it is the

accelerator constraints that suggest that the co-annihilation region is the allowed region.

As far as question (i) is concerned, one observes the following: In the mSUGRA models, at GUT scale we expect no degeneracies, the ΔM is large, since $m_{1/2}$ governs the gaugino masses, while m_0 the slepton masses. However, at the electroweak scale (EWS), the Renormalization Group Equation can modify this: e.g. the lightest selectron \tilde{e}^c at EWS has mass $m_{\tilde{e}^c}^2 = m_0^2 + 0.15m_{1/2}^2 + (37\text{GeV})^2$ while the $\tilde{\chi}_1^0$ has mass $m_{\tilde{\chi}_1^0}^2 = 0.16m_{1/2}^2$. The numerical accident that coefficients of $m_{1/2}^2$ is nearly the same for both cases allows a near degeneracy: for $m_0 = 0$, \tilde{e}^c and $\tilde{\chi}_1^0$ become degenerate at $m_{1/2} = (370-400)$ GeV. For larger $m_{1/2}$, near degeneracy is maintained by increasing m_0 to get the narrow corridor in m_0 - $m_{1/2}$ plane. Actually the case of the stau $\tilde{\tau}_1$ is more complicated⁴²: large t-quark mass causes left-right mixing in the stau mass matrix and this results in the $\tilde{\tau}_1$ being the lightest slepton and not the selectron. However, a result similar to the above occurs, with a $\tilde{\tau}_1 - \tilde{\chi}_1^0$ co-annihilation corridor appearing.

We note that the above results depend only on the U(1) gauge group and so co-annihilation can occur even if there were non-universal scalar mass soft-breaking or non-universal gaugino mass soft breaking at M_G . Thus, co-annihilation can occur in a wide class of SUGRA models, not just in mSUGRA. Hence, in such models one has naturally near degenerate neutralino-staus, and hence the answer to question (i) above is affirmative.

Now we come to the second important question (ii), namely, whether LHC measurements have the capability of asserting that the neutralino (if discovered) is the astrophysical DM. To this end we note that, in LHC, the

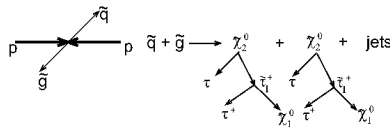


Figure 18. SUSY production of neutralinos and decay channels

major SUSY production processes of neutralinos are interactions of gluinos (\tilde{g}) and squarks (\tilde{q}) (c.f. figure 18), e.g., $p + p \rightarrow \tilde{g} + \tilde{q}$. These then decay into lighter SUSY particles. The final states involve two neutralinos $\tilde{\chi}_1^0$ giving rise to missing transverse energy (E_{miss}^T) and four τ 's, two from the \tilde{g} and two from the \tilde{q} decay chain for the example of fig. 18.

In the co-annihilation region, two of the taus have a high energy (“hard”

taus) coming from the $\tilde{\chi}_2^0 \rightarrow \tau\tilde{\tau}_1$ decay (since $M_{\tilde{\chi}_2^0} \simeq 2M_{\tilde{\tau}_1}$), while the other two are low energy particles (“soft” taus) coming from the $\tilde{\tau}_1 \rightarrow \tau + \tilde{\chi}_1^0$ decay, since ΔM is small.

The signal is thus $E_T^{\text{miss}} + \text{jets} + \tau$'s, which should be observable at the LHC detectors ⁴². As seen above, we expect two pairs of taus, each pair

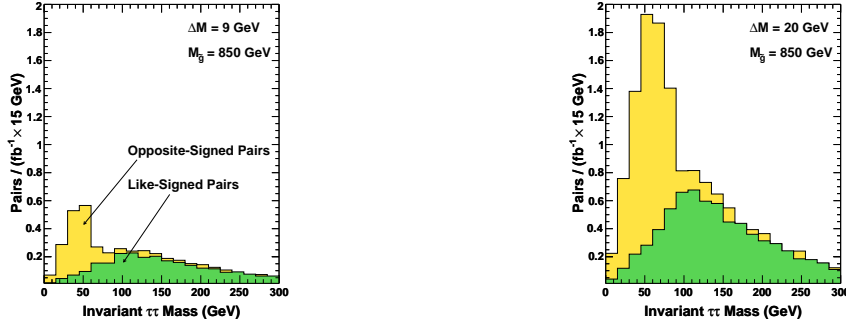


Figure 19. Number of tau pairs as a function of invariant $\tau\tau$ mass. The difference $N_{OS}-N_{LS}$ cancels for mass ≥ 100 GeV eliminating background events (from [42]).

containing one soft and one hard tau from each $\tilde{\chi}_2^0$ decay. Since $\tilde{\chi}_2^0$ is neutral, each pair should be of opposite sign. This distinguishes them from SM- and SUSY-backgrounds jets-faking taus, which will have equal number of like-sign as opposite-sign events ⁴². Thus, one can suppress backgrounds statistically by considering the number of opposite-sign events N_{OS} minus the like-sign events N_{LS} (figure 19).

The four τ final state has the smallest background but the acceptance and efficiency for reconstructing all four taus is low. Thus to implement the above ideas we consider here the three τ final state of which two are hard and one is soft. There are two important features: First, N_{OS-LS} increases with ΔM (since the τ acceptance increases) and N_{OS-LS} decreases with $M_{\tilde{g}}$ (since the production cross section of gluinos and squarks decrease with $M_{\tilde{g}}$). Second, one sees that N_{OS-LS} forms a peaked distribution. The di-tau peak position $M_{\tau\tau}^{\text{peak}}$ increases with both ΔM and $M_{\tilde{g}}$. This allows us to use the two observables N_{OS-LS} and $M_{\tau\tau}^{\text{peak}}$ to determine both ΔM and $M_{\tilde{g}}$ (c.f. figure 20). As becomes evident from the analysis ⁴² (c.f. fig. 21) it is possible to simultaneously determine ΔM and the gluino mass $M_{\tilde{g}}$. Moreover, one sees that at LHC even with 10 fb^{-1} (which should be available at the LHC after about two years running) one could determine

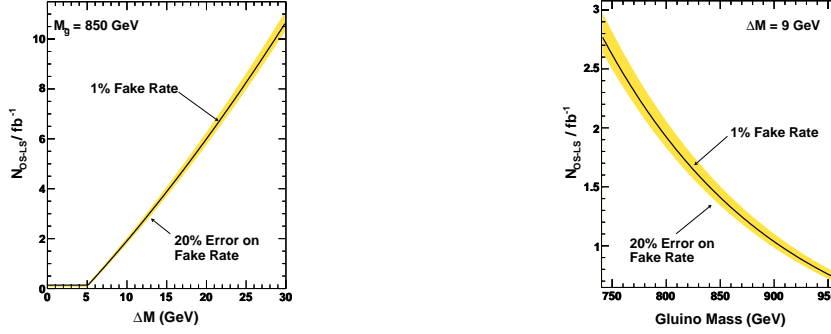


Figure 20. N_{OS-LS} as function of ΔM (left graph) and as a function of $M_{\tilde{g}}$ (right graph). The central black line assumes a 1% fake rate, the shaded area representing the 20% error in the fake rate (from [42]).

ΔM to within 22%, which should be sufficient to know whether one is in the SUGRA co-annihilation region. The above analysis was within the

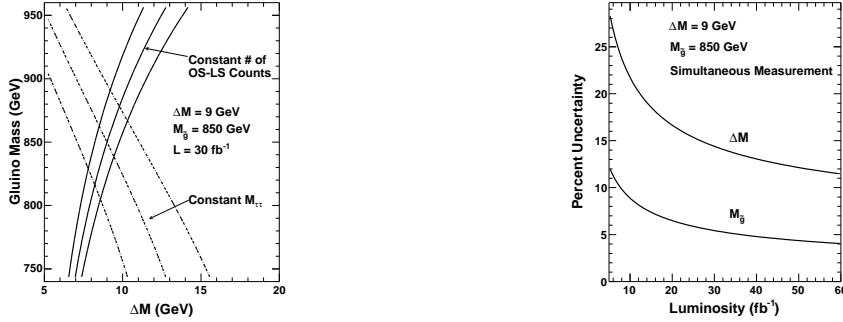


Figure 21. Left: Simultaneous determination of ΔM and $M_{\tilde{g}}$. The three lines plot constant N_{OS-LS} and $M_{\tilde{g}}^{\text{Peak}}$ (central value and 1σ deviation) in the $M_{\tilde{g}}-\Delta M$ plane for the benchmark point of $\Delta M=9$ GeV and $M_{\tilde{g}}=850$ GeV assuming 30 fb^{-1} luminosity. Right: Uncertainty in the determination of ΔM and $M_{\tilde{g}}$ as a function of luminosity (from [42]).

mSUGRA model, however similar analyses for other SUGRA models can be made, provided the production of neutralinos is not suppressed. In fact, the determination of $M_{\tilde{g}}$ depends on mSUGRA universality of gaugino masses at GUT scale, M_G , to relate $M_{\tilde{\chi}_2^0}$ to $M_{\tilde{g}}$ thus a model independent method

of determining $M_{\tilde{g}}$ would allow one to test the question of gaugino universality. However, it may not be easy to directly measure $M_{\tilde{g}}$ at the LHC for high $\tan\beta$ in the co-annihilation region due to the large number of low energy taus, and the ILC would require a very high energy option to see the gluino.

One can also measure ⁴² ΔM using the signal $E_T^{\text{miss}} + 2 \text{ jets} + 2\tau$. This signal has higher acceptance but larger backgrounds. With 10 fb^{-1} one can measure ΔM with 18% error at the benchmark point assuming a separate measurement of $M_{\tilde{g}}$ with 5% error has been made. While the benchmark point has been fixed in ⁴² at $M_{\tilde{g}} = 850 \text{ GeV}$ (i.e. $m_{1/2} = 360 \text{ GeV}$), higher gluino mass would require more luminosity to see the signal. One finds that with 100 fb^{-1} one can probe $m_{1/2}$ at the LHC up to $\sim 700 \text{ GeV}$ (i.e., $M_{\tilde{g}}$ up to $\simeq 1.6 \text{ TeV}$). Finally it should be mentioned that measurements of ΔM at the ILC could be made if a very forward calorimeter is implemented to reduce the two γ background. In such a case, ΔM can be determined with 10% error at the benchmark point, thereby implying that ⁴² in the co-annihilation region, the determination of ΔM at the LHC is not significantly worse than at the ILC.

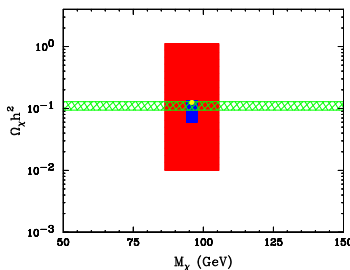


Figure 22. Accuracy of WMAP (horizontal green shaded region), LHC (outer red rectangle) and ILC (inner blue rectangle) in determining M_χ , the mass of the lightest neutralino, and its relic density $\Omega_\chi h^2$. The yellow dot denotes the actual values of M_χ and $\Omega_\chi h^2$ for a sample point in parameter space of mSUGRA: $m_0 = 57 \text{ GeV}$, $m_{1/2} = 250 \text{ GeV}$, $A_0 = 0$, $\tan\beta = 10$ and $\text{sign}(\mu) = +1$ (from A. Birkedal *et al.*, arXiv:hep-ph/0507214)

The results on the accuracy of determining DM mass in astrophysics and colliders within the mSUGRA framework is given in figure 22. We see that the cosmological measurement are at present the most accurate one, however, the reader should bear in mind the model-dependence of all these results. We now come to demonstrate this point by repeating the analysis

for some class of stringy models.

4.2. *Stringy Models and Particle Physics Constraints*

String theory (at least as we know it at present) lives in higher than four space-time dimensions (supersymmetric strings $D=10$). Low-energy field theory includes gravitational string multiplet fields (graviton, dilaton S (scalar), and supersymmetric partners in Supergravity theories). There is an obvious need for compactification to four dimensions. This happens dynamically through the Moduli scalar fields, T^i , of the string multiplets, which depend on the extra dimensions.

Originally, it was thought that the requirement of the absence of instabilities in the vacuum necessitates target-space supersymmetric strings (superstrings) in general. However, tachyonic instabilities may be welcome in cosmological scenarios, hence non supersymmetric target-space-time strings may be at play. Target-space supersymmetry needs breaking and must be phenomenologically consistent, i.e. partners must have masses above a few TeV. Consistent breaking of SUSY in string-inspired SUGRA via gaugino is possible, and rigorous, and phenomenologically realistic models, in this respect, do exist. It is the purpose of this subsection to discuss particle physics constraints in the framework of one class of such models. There are Modified Constraints on such string-inspired SUSY models from accelerator physics and Dark Matter which we shall discuss below.

The model we shall concentrate upon is a Heterotic string with Orbifold compactification from ten to four-dimensions with standard model gauge group $SU(3) \times SU(2) \times U(1)$, three generations, and consistent SUSY breaking via gaugino condensate⁹. Below we shall briefly review its most important features.

There is dominance of one-loop soft-SUSY-breaking *non-universal* terms, as a result of superconformal anomalies (non-zero β -function). This modifies predictions from mSUGRA, and implies an interpolation between Anomaly-Mediated SUSY Breaking models and mSUGRA. One distinguishes two regimes/scenarios for the SUSY-breaking terms:

Moduli-dominated: SUSY breaking is driven by the compactification moduli fields T^i , whose vacuum expectation value (v.e.v.) $\langle T^i \rangle \neq 0$ determines the size of the compact manifold. In this regime, there are light scalars and relatively heavy gauginos, whose nature depends completely on the value of the group-independent coefficient of the universal Green-Schwarz counterterm, δ_{GS} ⁹.

Dilaton-dominated: The dilaton S acquires a v.e.v. $\langle S \rangle \neq 0$, which in turn determines the value of string coupling g_s at the string scale, and transmits, via the (SUSY) auxiliary fields, SUSY Breaking. There are non-perturbative corrections to Kähler potential which stabilize the dilaton in the presence of gaugino condensation. The associated phenomenology is completely different from the moduli-dominated case. We are in a domain of heavy squarks and sleptons (of order of the gravitino scale) and *light gaugino masses*, driven by the dilaton auxiliary field v.e.v.'s

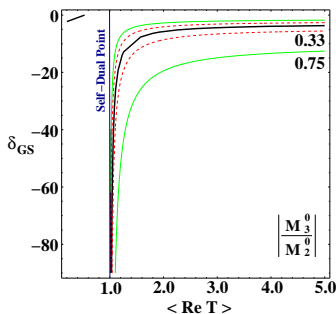


Figure 23. Contours of relative running gaugino masses M_3/M_2 in the $(\langle \text{Re } t \rangle, \delta_{\text{GS}})$ plane. These soft masses are at the initial (GUT) scale. The heavy (dark) contour is the limit of vanishing gluino mass (there is another such contour in the upper left corner on the other side of the self-dual point). For $\langle \text{Re } t \rangle > 1$ we also give contours of $|M_3/M_2| = 0.33$ (dashed) and 0.75 (solid).

There is a diverse origin of SUSY Breaking terms in this class of models: **(i)** Some come from the superconformal anomalies, and hence are non-universal (proportional to the β -function of the $SU(3) \times SU(2) \times U(1)$ groups); **(ii)** some are independent of the gauge group considered (Green-Schwarz counterterm, v.e.v. of the condensate). This interplay between universality and non-universality implies a *rich phenomenology*, new trends in the search of supersymmetric particles in accelerator and astro-particle physics.

The heterotic string models we shall analyze here make use of the so-called Pauli-Villars -Anomaly Mediated Supersymmetry Breaking (PV-AMSB) scenario⁹. There is an important feature of the AMSB-string models which turns out to be important for DM searches, namely the presence of *non-thermal* LSP relic densities. Indeed, in AMSB studies it was found that the neutralino thermal relic density is generically too small to explain the amount of dark matter: the wino content of the LSP is quite high.

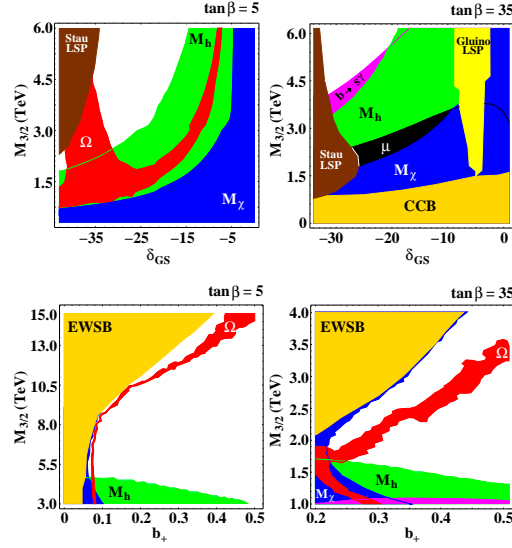


Figure 24. Upper: Constraints on the moduli-dominated parameter space for $\tan\beta = 5$ (left) and $\tan\beta = 35$ (right) with $p = 0$ and $\langle \text{Re } t \rangle = 2.0$. Constraints on the $(M_{3/2}, \delta_{\text{GS}})$ plane are given for $\mu > 0$. The dark shaded regions on the left have a stau LSP. The $\tan\beta = 35$ plot also has a region with a gluino LSP. For $\tan\beta = 5$ the region labeled “ Ω ” has the cosmologically preferred relic density of neutralinos. No such region exists for the higher $\tan\beta$ plot. In that case the exclusion contours are due to (from bottom right to upper left) Charge Conjugation Breaking vacua, the chargino mass, too large SUSY contributions to $(g_\mu - 2)$, the Higgs mass limit and too large a $b \rightarrow s\gamma$ rate. Lower: Constraints on the dilaton-dominated parameter space for $\tan\beta = 5$ (left) and $\tan\beta = 35$ (right). Constraints on the $(M_{3/2}, b_+)$ plane are given for $\mu > 0$ [with b_+ the largest β -function coefficient among condensing gauge groups of the hidden sector].

Additionally, co-annihilation between the LSP and the lightest chargino is also very efficient. Both of these effects combine to make the thermal relic density of LSP negligible. Thus the anomaly-mediated character of the gaugino sector in this model necessitates a non-thermal production mechanism for neutralino LSPs, or another candidate for the cold dark matter must be postulated.

We next remark that, in the moduli-domination scenario of the heterotic string models, the various Kähler moduli are not stabilized, i.e. $\langle \text{Re } t \rangle$ is not fixed, and one must use the soft terms. The value of the Green-Schwarz coefficient δ_{GS} , then, becomes relevant for the determination of gaugino masses⁹, which are “running” with it (c.f. figure 23).

The relevant astro-particle physics constraints for one indicative exam-

ple of heterotic orbifold models ⁹, in some range of the parameter space, are summarized in figure 24. The reader’s attention is drawn to the strong suppression (or disappearance) of thermal neutralino relic densities in some regions of the parameter space.

4.3. *Non-critical (non-equilibrium) Stringy Q-Cosmology*

The results described on the previous sub section were based on a critical string theory, where the dilaton field is stabilized. However, one may encounter situations in some non-equilibrium stringy cosmologies, described by non-critical strings ¹⁰ (Q-cosmologies), in which the dilaton is not stabilized. Such cosmologies might arise, for instance, in colliding brane world scenarios, where the cosmically catastrophic early universe event of collision suffices to induce departure of the associated string theory, describing various excitations on our brane world, from conformal invariance (on a world sheet) and hence non-criticality. In such models, the dilatons are time dependent and are not stabilized. At late eras of the Universe, such a time dependent dilaton may behave as quintessence-like field leading to acceleration of the Universe ^{43,10,17}. The departure of criticality has also other consequences for the low-energy field theory, namely the existence of off-shell terms ¹⁰, i.e. the variations of the relevant effective action with respect to the fields in the gravitational string multiplet (gravitons, dilatons) may be non zero. A detailed analysis ⁴⁴ shows that in such models, where the dilaton is not stabilized, it is possible to have thermal relic abundances of DM particles, such as neutralinos in supersymmetric cases, whose density, however, obeys a *modified* Boltzmann equation by the dilaton and off-shell source terms:

$$\frac{dn}{dt} + 3 \left(\frac{\dot{a}}{a} \right) n = \dot{\Phi} n - \frac{1}{2} \left(e^{-\Phi} g^{\mu\nu} \tilde{\beta}_{\mu\nu}^{\text{Grav}} + 2e^{\Phi} \tilde{\beta}^{\Phi} \right) n + \int \frac{d^3p}{E} C[f] \quad (4.14)$$

with $n = \int d^3p f$ the species number density. The β -terms denote the off-shell terms in the gravitational (graviton, dilaton) multiplet of the string: $\tilde{\beta}_{\mu\nu}^{\text{Grav}} \propto \frac{\delta S}{\delta g^{\mu\nu}}$, $\tilde{\beta}^{\Phi} \propto \frac{\delta S}{\delta \Phi} \neq 0$, where S is the low-energy string-inspired target-space effective action.

If we set, for brevity, $\Gamma(t) \equiv \dot{\Phi} - \frac{1}{2} \left(e^{-\Phi} g^{\mu\nu} \tilde{\beta}_{\mu\nu}^{\text{Grav}} + 2e^{\Phi} \tilde{\beta}^{\Phi} \right)$, acting as a source term on the right-hand-side of the Boltzmann equation (4.14), then we can solve this equation to obtain for the thermal DM relic abundance

(assuming a single species, e.g. neutralino $\tilde{\chi}$)⁴⁴:

$$\Omega_{\tilde{\chi}} h_0^2 = (\Omega_{\tilde{\chi}} h_0^2)_{no-source} \times \left(\frac{\tilde{g}_*}{g_*} \right)^{1/2} \exp \left(\int_{x_0}^{x_f} \frac{\Gamma H^{-1}}{x} dx \right) \quad (4.15)$$

with $(\Omega_{\tilde{\chi}} h_0^2)_{no-source}$ the standard (equilibrium) cosmology result (3.10); the star notation denotes quantities at the freeze-out point, $\tilde{g} = g + \frac{30}{\pi^2} T^{-4} \Delta\rho$, with T the temperature, g is the effective number of (thermal) degrees of freedom in this non-critical string Universe and $\Delta\rho$ denotes collectively the dilaton and off-shell (due to the β -functions) terms in the effective modified Friedman equation of the Q-cosmology^{10,44}: $H^2 = \frac{8\pi G_N}{3} (\rho + \Delta\rho)$.

Depending on their signature, the Source Terms Γ have different influence on the relic abundance, with profound consequences on the prospects for detecting supersymmetry in such models at colliders. For instance, for a given model⁴⁴ and within a certain region of the parameters, there is a reduction of neutralino relic abundance, as compared with conventional cosmologies, by a factor of about 1/10 (c.f. figure 25), leading to a relaxation on some of the constraints regarding SUSY detection prospects at LHC imposed by mSUGRA models.

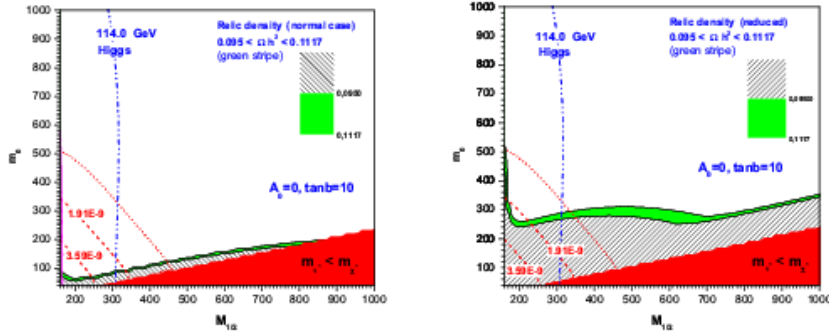


Figure 25. Left: In the thin green (grey) stripe the neutralino relic density is within the WMAP3 limits for values $A_0 = 0$ and $\tan\beta = 10$, according to the source-free $\Gamma = 0$ *conventional Cosmology*. The dashed lines (in red) are the 1σ boundaries for the allowed region by the $g-2$ muon's data as shown in the figure. The dotted lines (in red) delineate the same boundaries at the 2σ 's level. In the hatched region $0.0950 > \Omega_{CDM} h^2$, while in the dark (red) region at the bottom the LSP is a stau. Right: The same as in left panel, but according to the non-critical-string calculation, in which the relic density is reduced in the presence of dilaton sources $\Gamma = \dot{\phi} \neq 0$.

5. Conclusions and Looking Ahead

In this set of lectures I have reviewed various astrophysical methods for constraining the Universe energy budget, and used such results to constrain interesting particle physics models of cosmological relevance. I have discussed the issue of calculating thermal-relic DM abundances in those models, with the intention of placing constraints on interesting particle physics models, such as supersymmetry, exploiting astrophysical data. I mainly concentrated on DM searches at LHC. I came to the conclusion that LHC could shed some light on the issue as to whether the astronomically observed DM is the neutralino, but this is a highly model dependent statement. I have analyzed briefly the phenomenology of various SUGRA models (mSUGRA, and some string inspired ones, including some relaxation non-equilibrium dilaton-quintessence models). The associated phenomenologies are very different, depending crucially on the details of the underlying dynamics, such as the type of the SUGRA model, the way of SUSY breaking *etc.* There are model independent methods for testing DM at colliders, but they pertain to subdominant processes at colliders.

For future directions it would be desirable to explore in more detail SUSY models with *CP violation*, which recently started attracting attention ⁴⁵, since, due to bounds on Higgs $m_H > 114$ GeV, we now know that the amount of CP Violation in the Standard Model is not sufficient to generate the observed baryon asymmetry of the Universe ⁴⁶, and hence SUSY CP violation might play an important rôle in this respect. At this point I mention that parameters in SUGRA models that can have CP phases are the gaugino and higgsino masses and trilinear sfermion-Higgs couplings. CP phases affect co-annihilation scenaria, and hence the associated particle physics dark matter searches at colliders ⁴⁵. Another direction is to constrain SUSY GUTs models (e.g. flipped SU(5)) using astrophysical data ⁷, after taking, however, proper account of the observed dark energy in the Universe. Personally, I believe that this dark energy is due to some quintessence (relaxing to zero (non-equilibrium) field). WMAP data point towards an equation of state of quintessence type, $w = p/\rho \rightarrow -1$ (close to that of a cosmological constant, but not quite -1). Such features may be shared by dilaton quintessence, as discussed briefly above in the context of string theory. The issue is, however, still wide open and constitutes one of the pressing future directions for theoretical research in this field.

On the experimental side, LHC and future (linear) collider, but also direct ²³, dark matter searches could shed light on the outstanding issue

of the nature of the Cosmological Dark Sector (especially Dark Matter), but one has to bear in mind that such searches are highly theoretical-model dependent. To such ideas one should also add the models invoking Lorentz violation as alternative to dark matter. Clearly, particle physics can play an important rôle in constraining such alternative models in the future, especially in view of the upcoming high-precision terrestrial and extraterrestrial experiments, such as Auger, Planck mission, high-energy neutrino astrophysics *etc.*

Nothing is certain, of course, and careful interpretations of possible results are essential. Nevertheless, the future looks promising, and certainly particle physics and astrophysics will proceed together and provide a fruitful and complementary experience to each other and exchange interesting sets of ideas for the years to come.

Acknowledgments

I would like to thank the organizers of the Lake Louise Winter Institute 2007 (Lake Louise (Canada), February 19-24 2007) for the invitation and support and for providing such a successful and thought-stimulating meeting. This work is partially supported by the European Union through the Marie Curie Research and Training Network *UniverseNet* MRTN-CT-2006-035863.

References

1. B. P. Schmidt *et al.*, *Astrophys. J.* **507** (1998) 46; S. Perlmutter *et al.* [Supernova Cosmology Project Collaboration], *Astrophys. J.* **517** (1999) 565; A. G. Riess *et al.*, *Astrophys. J.* **560** (2001) 49.
2. S. Perlmutter and B. P. Schmidt, arXiv:astro-ph/0303428; J. L. Tonry *et al.*, arXiv:astro-ph/0305008; P. Astier *et al.*, *Astron. Astrophys.* **447** (2006) 31. A. G. Riess *et al.*, *Astrophys. J.* **659** (2007) 98. W. M. Wood-Vasey *et al.*, arXiv:astro-ph/0701041.
3. C. L. Bennett *et al.*, arXiv:astro-ph/0302207.
4. D. J. Eisenstein *et al.* [SDSS Collaboration], *Astrophys. J.* **633**, 560 (2005).
5. G. F. Smoot *et al.*, *Astrophys. J.* **396**, L1 (1992); C. L. Bennett *et al.*, *Astrophys. J.* **436**, 423 (1994).
6. D. N. Spergel *et al.* [WMAP Collaboration], *Astrophys. J. Suppl.* **148**, 175 (2003); **170**, 377 (2007).
7. A. B. Lahanas, N. E. Mavromatos and D. V. Nanopoulos, *Int. J. Mod. Phys. D* **12**, 1529 (2003), and references therein.
8. A. H. Chamseddine, R. Arnowitt and P. Nath, *Phys. Rev. Lett.* **49** (1982) 970; R. Barbieri, S. Ferrara and C. A. Savoy, *Phys. Lett. B* **119** (1982) 343; L. J. Hall, J. Lykken and S. Weinberg, *Phys. Rev. D* **27** (1983) 2359; P. Nath, R. Arnowitt and A. H. Chamseddine, *Nucl. Phys. B* **227** (1983) 121.

9. P. Binetruy *et al.*, Eur. Phys. J. C **47**, 481 (2006); P. Binetruy, M. K. Gaillard and B. D. Nelson, Nucl. Phys. B **604**, 32 (2001).
10. J. R. Ellis *et al.*, Int. J. Mod. Phys. A **21**, 1379 (2006), and references therein. G. A. Diamandis *et al.*, Phys. Lett. B **642**, 179 (2006).
11. S. Eidelman, talk at ICHEP 2006, Moscow (Russia).
12. E. Kolb and M. Turner, *The Early Universe* (Frontiers in Physics, Addison-Wesley, 1989).
13. H. V. Peiris *et al.*, arXiv:astro-ph/0302225; V. Barger, H. S. Lee and D. Marfatia, Phys. Lett. B **565**, 33 (2003).
14. A. Kosowsky and M. S. Turner, Phys. Rev. D **52**, 1739 (1995).
15. E. W. Kolb, S. Matarrese and A. Riotto, New J. Phys. **8** 322 (2006).
16. V. A. Mitsou, these proceedings [arXiv:0708.0113 [astro-ph]], and references therein; J. R. Ellis, *et al.*, Astropart. Phys. **27**, 185 (2007); N. E. Mavromatos and V. A. Mitsou, arXiv:0707.4671 [astro-ph].
17. M. Gasperini, Phys. Rev. D **64**, 043510 (2001); M. Gasperini, F. Piazza and G. Veneziano, Phys. Rev. D **65**, 023508 (2002); R. Bean and J. Magueijo, Phys. Lett. B **517**, 177 (2001).
18. M. Milgrom, Astrophys. J. **270**, 365 (1983).
19. J. D. Bekenstein, Phys. Rev. D **70**, 083509 (2004) [Erratum-ibid. D **71**, 069901 (2005)].
20. C. Skordis *et al.*, Phys. Rev. Lett. **96**, 011301 (2006).
21. S. Dodelson and M. Liguori, Phys. Rev. Lett. **97**, 231301 (2006).
22. E. Gravanis and N. E. Mavromatos, Phys. Lett. B **547**, 117 (2002).
23. V. Zacek, these proceedings and references therein.
24. F. Zwicky, Helv. Phys. Acta **6**, 110 (1933).
25. M. Tegmark *et al.* [SDSS Collaboration], Astrophys. J. **606**, 702 (2004).
26. J. R. Ellis, *et al.*, Nucl. Phys. **B238** (1984) 453; H. Goldberg, Phys. Rev. Lett. **50** (1983) 1419.
27. N. Yoshida, *et al.*, Astrophys. J. **591**, L1 (2003).
28. J. R. Ellis, J. L. Lopez and D. V. Nanopoulos, Phys. Lett. B **247** (1990) 257; J. R. Ellis, *et al.*, Nucl. Phys. B **373** (1992) 399. S. Sarkar, arXiv:hep-ph/0005256 and references therein.
29. D. J. Chung, Phys. Rev. D **67** (2003) 083514.
30. J. R. Ellis, T. Falk, K. A. Olive and M. Srednicki, Astropart. Phys. **13** (2000) 181 [Erratum-ibid. **15**, 413 (2001)].
31. A. Birkedal, AIP Conf. Proc. **805**, 55 (2006) and references therein.
32. U. Chattopadhyay, A. Corsetti and P. Nath, Phys. Rev. D **68**, 035005 (2003); K. L. Chan, U. Chattopadhyay and P. Nath, Phys. Rev. D **58**, 096004 (1998).
33. J. Edsjo and P. Gondolo, Phys. Rev. D **56**, 1879 (1997).
34. J. L. Feng, K. T. Matchev and T. Moroi, Phys. Rev. Lett. **84**, 2322 (2000); Phys. Rev. D **61**, 075005 (2000).
35. H. Baer and C. Balazs, JCAP **0305**, 006 (2003).
36. G. W. Bennett *et al.* [BNL-E821 Collaboration], Phys. Rev. Lett. **89** (2002) 101804; C. J. Onderwater *et al.* [BNL-E821 Collaboration], AIP Conf. Proc. **549**, 917 (2002).
37. S. Narison, Phys. Lett. B **568**, 231 (2003).

38. J. R. Ellis, *et al.*, Phys. Lett. B **565**, 176 (2003).
39. A. B. Lahanas and D. V. Nanopoulos, Phys. Lett. B **568**, 55 (2003).
40. H. Baer, *et al.*, JHEP **0306**, 054 (2003).
41. H. Baer, T. Krupovnickas and X. Tata, JHEP **0307**, 020 (2003).
42. R. Arnowitt *et al.*, arXiv:hep-ph/0701053 and references therein.
43. G. A. Diamandis, *et al.* Int. J. Mod. Phys. A **17**, 4567 (2002);
44. A. B. Lahanas, N. E. Mavromatos and D. V. Nanopoulos, Phys. Lett. B **649**, 83 (2007); arXiv:hep-ph/0608153, Phys. Math. Central, Physics A, in press.
45. G. Belanger, *et al.*, AIP Conf. Proc. **878**, 46 (2006); Phys. Rev. D **73**, 115007 (2006).
46. A. Pilaftsis and C. E. M. Wagner, Nucl. Phys. B **553**, 3 (1999).